JAERI-M
93-020

NEUTRON-PHOTON MULTIGROUP CROSS SECTIONS FOR NEUTRON ENERGIES UP TO 400 MEV : HILO86R
- REVISION OF HILO86 LIBRARY -

February 1993

Hiroshi KOTEGAWA, Yoshihiro NAKANE,
Akira HASEGAWA and Shun-ichi TANAKA

日 本 原 子 力 研 究 所
Japan Atomic Energy Research Institute

編集兼発行　日本原子力研究所

印　　刷　ニッセイエブロ株式会社

Neutron-photon Multigroup Cross Sections for
Neutron Energies Up to 400 MeV: HILO86R
- Revision of HILO86 Library -

Hiroshi KOTEGAWA, Yoshihiro NAKANE, Akira HASEGAWA
and Shun-ichi TANAKA

Department of Reactor Engineering
Tokai Research Establishment
Japan Atomic Energy Research Institute
Tokai-mura, Naka-gun, Ibaraki-ken

(Received January 18, 1993)

A macroscopic multigroup cross section library of 66 neutron and 22 photon groups for neutron energies up to 400MeV: HILO86R is prepared for 10 typical shielding materials; water, concrete, iron, air, graphite, polyethylene, heavy concrete, lead, aluminum and soil. The library is a revision of the DLC-119/HILO86, in which only the cross sections below 19.6 MeV have been exchanged with a group cross section processed from the JENDL-3 microscopic cross section library. In the HILO86R library, self shielding factors are used to produce effective cross sections for neutrons less than 19.6 MeV considering rather coarse energy meshes.

Energy spectra and dose attenuation in water, concrete and iron have been compared among the HILO, HILO86 and HILO86R libraries for different energy neutron sources. Significant discrepancy has been observed in the energy spectra less than a couple of MeV energy in iron among the libraries, resulting large difference in the dose attenuation. The difference was attributed to the effect of self-shielding factor, namely to the difference between infinite dilution and effective cross sections. Even for 400 MeV neutron source the influence of the self-shielding factor is significant, nevertheless only the cross sections below 19.6 MeV are exchanged.

Keywords: DLC-87/HILO, DLC-119/HIL086, HIL086R, 400MeV Neutron Source, Group Cross Section, Self-shielding Factor, JENDL-3

400 MeV までの中性子に対する、中性子－光子多群断面積ライブラリー：ＨＩＬＯ８６Ｒ
－ ＨＩＬＯ８６ライブラリーの改訂 －

日本原子力研究所東海研究所原子炉工学部
小手川　洋・中根　佳弘・長谷川　明・田中　俊一

（1993 年 1 月 18 日受理）

巨視的多群断面積ライブラリーＨＩＬＯ８６Ｒとして、代表的遮蔽材である、水、普通コンクリート、鉄、空気、グラファイト、ポリエチレン、重コンクリート、鉛、アルミニュウム、土の10物質に対し、断面積を作成した。このライブラリーは、DLC－119/ＨＩＬＯ８６の改訂版であり、19.6 MeV 以下の断面積を、ＪＥＮＤＬ－３ 微視的断面積ライブラリーを処理して作った断面積と置き換えたものである。本ライブラリーは、エネルギーメッシュの粗い事に注意し、自己遮蔽因子を考慮した実効断面積となっている。

水、コンクリート、鉄中の、いくつかのエネルギー中性子線源による中性子のエネルギースペクトルと線量当量減衰率に関して、ＨＩＬＯ, ＨＩＬＯ８６とＨＩＬＯ８６Ｒとの間で比較を行った。鉄中での、数 MeV 以下のエネルギースペクトルに顕著な差が認められ、その影響は、線量当量減衰率に対しても、大きな差となって現れる。19.6 MeV 以下の断面積の影響が、400 MeV 中性子線源に対する線量当量減衰率の場合に置いて、無視できない事が示された。

東海研究所：〒 319－11　茨城県那珂郡東海村白方字白根 2 － 4

Contents

目　　次

1. Introduction

Multigroup cross sections have been widely used for shielding calculations of nuclear facilities with discrete ordinates codes and Monte Carlo codes such as ANISN, DOT, MORSE, and so forth. Very few group cross sections, however, are available for neutron energies higher than 20 MeV. Alsmiller et al. initially presented neutron-photon multigroup cross sections DLC58/HELLO[1] for neutrons up to 60 MeV, and expaneded the data up to 400 MeV as DLC87/HILO.[2] The HILO library has been revised as DLC119/HILO86[3] in 1986, however the newer data had been classified for Japan untill 1991. Therefore, only the HILO library has been available data for us, so far.

After having the newest libray HILO86, we have made several test calculations with the ANISN code, and noticed serious discrepancy, especially in the neutron dose attenuation in iron from the calculated results using the JSD100[4] for a ^{252}Cf neutron source, although the results with the JSD100 have already been verified in comparing with measurements and other calculations. This is the incentive of the present work to revise the HILO86 data.

In this report, the detail of the HILO86R cross sections is described, and the calculations with respect to energy spectra and dose attenuations are compared for the HILO86 and HILO86R libraries with together the results of the HILO and JSD100.

2. HILO86R Library

Group cross sections for the ten materials listed in Table 1 were prepared in the HILO86R library. The energy group boundaries of the cross sections are shown in Tables 2 and 3. The atomic number densities of the materials are given in Table 4.

2.1 Cross sections above 19.6 MeV

The cross sections above 19.6MeV are the copy of HILO86, therefore, the energy group structure and P_5 Legendre expansion is not changed.

1. Introduction

Multigroup cross sections have been widely used for shielding calculations of nuclear facilities with discrete ordinates codes and Monte Carlo codes such as ANISN, DOT, MORSE, and so forth. Very few group cross sections, however, are available for neutron energies higher than 20 MeV. Alsmiller et al. initially presented neutron-photon multigroup cross sections DLC58/HELLO[1] for neutrons up to 60 MeV, and expaneded the data up to 400 MeV as DLC87/HILO.[2] The HILO library has been revised as DLC119/HILO86[3] in 1986, however the newer data had been classified for Japan untill 1991. Therefore, only the HILO library has been available data for us, so far.

After having the newest libray HILO86, we have made several test calculations with the ANISN code, and noticed serious discrepancy, especially in the neutron dose attenuation in iron from the calculated results using the JSD100[4] for a ^{252}Cf neutron source, although the results with the JSD100 have already been verified in comparing with measurements and other calculations. This is the incentive of the present work to revise the HILO86 data.

In this report, the detail of the HILO86R cross sections is described, and the calculations with respect to energy spectra and dose attenuations are compared for the HILO86 and HILO86R libraries with together the results of the HILO and JSD100.

2. HILO86R Library

Group cross sections for the ten materials listed in Table 1 were prepared in the HILO86R library. The energy group boundaries of the cross sections are shown in Tables 2 and 3. The atomic number densities of the materials are given in Table 4.

2.1 Cross sections above 19.6 MeV

The cross sections above 19.6MeV are the copy of HILO86, therefore, the energy group structure and P_5 Legendre expansion is not changed.

2.2 Cross sections below 19.6 MeV

Neutron cross sections of 37 energy groups less than 19.6MeV have been collapsed from 295-neutron and 104-photon JSSTDL library[5] based on JENDL-3 cross section library[6], considering self-shielding factors. The JSSTDL data library is composed of infinite dilution cross sections produced with the weighting spectra of 1/E above thermal neutrons and Maxwell distribution for thermal neutrons, and of Bondarenko type self-shielding factors[7] processed with the Prof-GROUCH-G/B code system.[8] Further, a set of infinite dilution group cross sections and corresponding self-shielding factors with the same group structure with that of HILO86R have been condensed from the JSSTDL cross sections using the CONDENS-MACRO-JG in the JSSTDL system.[9] Finally, macroscopic effective cross sections for the HILO86R library were obtained as the products of these data for each material.

In Figs.1 to 10, total cross sections of HILO86R library are demonstrated for 10 kinds of materials, respectively, in which effective and infinite dilution cross sections are compared. The difference between both cross sections is fairly large in resonance energy region because of large self-shielding factor as seen typically for iron and aluminum in Figs.3 and 9.

2.3 Photon cross sections

Photon cross sections for tranport calculations also have been condensed from the JSSTDL library using a flat weighting spectrum. While, secondary gamma-ray production cross sections have not changed with those in the HILO86 library.

3. Comparison of Cross Sections among HILO, HILO86 and HILO86R

Cross sections below 19.6 MeV in the HILO and HILO86 libraries have been collapsed from the VITAMIN-C[10] based on ENDF/B-IV[11] and the VITAMIN-E[12] on ENDF/B-V[13], respectively, and the collapsion procedure were different from each other and also from that for HILO86R.

2.2 Cross sections below 19.6 MeV

Neutron cross sections of 37 energy groups less than 19.6MeV have been collapsed from 295-neutron and 104-photon JSSTDL library[5] based on JENDL-3 cross section library[6], considering self-shielding factors. The JSSTDL data library is composed of infinite dilution cross sections produced with the weighting spectra of 1/E above thermal neutrons and Maxwell distribution for thermal neutrons, and of Bondarenko type self-shielding factors[7] processed with the Prof-GROUCH-G/B code system.[8] Further, a set of infinite dilution group cross sections and corresponding self-shielding factors with the same group structure with that of HILO86R have been condensed from the JSSTDL cross sections using the CONDENS-MACRO-JG in the JSSTDL system.[9] Finally, macroscopic effective cross sections for the HILO86R library were obtained as the products of these data for each material.

In Figs.1 to 10, total cross sections of HILO86R library are demonstrated for 10 kinds of materials, respectively, in which effective and infinite dilution cross sections are compared. The difference between both cross sections is fairly large in resonance energy region because of large self-shielding factor as seen typically for iron and aluminum in Figs.3 and 9.

2.3 Photon cross sections

Photon cross sections for tranport calculations also have been condensed from the JSSTDL library using a flat weighting spectrum. While, secondary gamma-ray production cross sections have not changed with those in the HILO86 library.

3. Comparison of Cross Sections among HILO, HILO86 and HILO86R

Cross sections below 19.6 MeV in the HILO and HILO86 libraries have been collapsed from the VITAMIN-C[10] based on ENDF/B-IV[11] and the VITAMIN-E[12] on ENDF/B-V[13], respectively, and the collapsion procedure were different from each other and also from that for HILO86R.

Comparison of the three kinds of libraries are shown for total cross sections of water, ordinary concrete, and iron in Figs.11 to 13. All of cross sections for water are agreed except for thermal neutron group, while for iron and ordinary concrete quite large difference is observed, especially for iron. For iron, the peak cross section around 26 keV (54 group) in the HILO and HILO86 becomes a valley one in the HILO86R because of the large self-shielding factor. Fig.14 is a comparison of total cross sections among the HILO, HILO86 and the infinite dilution cross section in HILO86R. The comparison suggests that the HILO cross section is nearly equal to the infinite dilution cross section of HILO86R, and the HILO86 cross section, which was collapsed with ANISN using a source characteristic of a fusion spectrum as specified by Santoro et al.[14], is rather consistent with the infinite dilute cross section than the effective one in the HILO86R.

4. Transport Calculations

4.1 Energy spectrum

Energy spectra in water, iron for ^{252}Cf source with the JSD100 cross section are compared with those with HILO86R and HILO86 in Figs.15 and 16, which were calculated with ANISN-JR in a spherical geometry. The results with the JSD100 and the HILO86R are in reasonable agreement, while the discreancy with the HILO86 is very serious in iron. As the JSD100 cross sections based on ENDF/B-IV are effective one considering self-shielding factors, the discrepancy with the HILO86 is attributed to the effect of self-shielding factors. Next, energy spectra in iron and ordinary concrete for ^{252}Cf, 50 MeV, and 400 MeV neutron sources have been calculated using HILO86R, HILO86 and HILO cross sections, and compared as shown in Figs.17 to 22. Difference in iron is remarkable in energy region less than about 10 MeV even for neutron sources higher than 19.6 MeV neutrons, and increases significantly with penetration.

Comparison of the three kinds of libraries are shown for total cross sections of water, ordinary concrete, and iron in Figs.11 to 13. All of cross sections for water are agreed except for thermal neutron group, while for iron and ordinary concrete quite large difference is observed, especially for iron. For iron, the peak cross section around 26 keV (54 group) in the HILO and HILO86 becomes a valley one in the HILO86R because of the large self-shielding factor. Fig.14 is a comparison of total cross sections among the HILO, HILO86 and the infinite dilution cross section in HILO86R. The comparison suggests that the HILO cross section is nearly equal to the infinite dilution cross section of HILO86R, and the HILO86 cross section, which was collapsed with ANISN using a source characteristic of a fusion spectrum as specified by Santoro et al.[14], is rather consistent with the infinite dilute cross section than the effective one in the HILO86R.

4. Transport Calculations

4.1 Energy spectrum

Energy spectra in water, iron for ^{252}Cf source with the JSD100 cross section are compared with those with HILO86R and HILO86 in Figs.15 and 16, which were calculated with ANISN-JR in a spherical geometry. The results with the JSD100 and the HILO86R are in reasonable agreement, while the discreancy with the HILO86 is very serious in iron. As the JSD100 cross sections based on ENDF/B-IV are effective one considering self-shielding factors, the discrepancy with the HILO86 is attributed to the effect of self-shielding factors. Next, energy spectra in iron and ordinary concrete for ^{252}Cf, 50 MeV, and 400 MeV neutron sources have been calculated using HILO86R, HILO86 and HILO cross sections, and compared as shown in Figs.17 to 22. Difference in iron is remarkable in energy region less than about 10 MeV even for neutron sources higher than 19.6 MeV neutrons, and increases significantly with penetration.

4.2 Attenuation

With the energy spectra, dose equivalent attenuation in ordinary concrete and iron were also examined for ^{252}Cf neutron, and 10, 50, 200 and 400 MeV monoenergetic neutron sources under the same calculational conditions as shown in Figs.23 to 32, where the conversion factors from fluence to dose equivalent were taken from ICRP Publication-51[15]. Small difference is seen for ^{252}Cf and 10 MeV sources, but the influence of the different cross sections is marginal for ordinary concrete. On the other hand, the difference is very large for iron, and the influence of the different cross sections less than 19.6 MeV is significant even for 400 MeV neutron source.

5. Summary

A neutron-photon macroscopic cross section library HILO86R for high energy neutron shielding calculations has been presented by revising the cross section below 19.6 MeV in the HILO86 library. Comprehensive comparisons between the HILO86R with other libraries HILO86, HILO and JSD100 made clear the significant effect of self-shielding factors in resonance energy region.

4.2 Attenuation

With the energy spectra, dose equivalent attenuation in ordinary concrete and iron were also examined for ^{252}Cf neutron, and 10, 50, 200 and 400 MeV monoenergetic neutron sources under the same calculational conditions as shown in Figs.23 to 32, where the conversion factors from fluence to dose equivalent were taken from ICRP Publication-51[15]. Small difference is seen for ^{252}Cf and 10 MeV sources, but the influence of the different cross sections is marginal for ordinary concrete. On the other hand, the difference is very large for iron, and the influence of the different cross sections less than 19.6 MeV is significant even for 400 MeV neutron source.

5. Summary

A neutron-photon macroscopic cross section library HILO86R for high energy neutron shielding calculations has been presented by revising the cross section below 19.6 MeV in the HILO86 library. Comprehensive comparisons between the HILO86R with other libraries HILO86, HILO and JSD100 made clear the significant effect of self-shielding factors in resonance energy region.

References

1) Alsmiller R.G.,Jr. and Braish J.:"Neutron-Photon Multigroup Cross Sections for Neutron Energies $\leq$ 60MeV",ORNL/TM-6486(1978).
2) Alsmiller R.G.,Jr. and Barish J.:"Neutron-Photon Multigroup Cross Sections for Neutron Energies $\leq$ 400MeV",ORNL/TM-7818(1981).
3) Alsmiller R.G.,Jr., Barnes J.M. and Drischler J.D.:"Neutron-Photon Multigroup Cross Sections for Neutron Energies $\leq$ 400MeV(Revision 1)",ORNL/TM-9801(1986).
4) ORNL-RSIC Data Library Collection, DLC-51/JSD-100/120.
5) Hasegawa A.:"Development of a Common Nuclear Group Constants Library System: JSSTDL-295n-104γ Based on JENDL-3 Nuclear Data Library",Nuclear Data Science and Technology, pp.232 Springer Verlag(1991).
6) Shibata K., Nakagawa T. and Asami T.:"Japanese Evaluated Nuclear Data Library, Version-3;JENDL-3",JAERI-1319(1990).
7) Abagyan L.P. et al.,:"Group Constants for Nuclear Reactor Constants", Consultants Bureau, N.Y.(1964).
8) Hasegawa A.:"Development of a Processing Code System Prof. GROUCH-G/B", unpublished work(1986).
9) Hasegawa A.:"CONDENS-MACRO-JG", unpublished work(1986).
10) "VITAMIN-C, 171 Neutron, 36 Gamma Ray Group Cross Sections in AMPX and CCCC Interface Formats for Fusion and LMFBR Neutronics", Radiation Shielding Information Center, DLC-41(1977).
11) Garber D.(editor):"ENDF/B-IV",ENDF/B Summary Documantation ENDF-201 (2nd Edition) NNDC.,BNL(1975).
12) Weisbin C.R., Roussin R.W. and et al.:"VITAMIN-E: An ENDF/B-V Multigroup Cross-Section Library for LMFBR Core and Shield, LWR Shield, Dosimetry and Fusion Blanket Technology",ORNL-5505(ENDF-274)(1979).
13) Garber D.(editor):"ENDF/B-V",Report BNL-17541(ENDF-201), National Nuclear Data Laboratory(1979).
14) Santoro R.T., Roussin R.W. and Barnes J.M.:"FLUNG:Coupled 35-Group Neutron and 21-Group Gamma Ray, P_3 Cross Sections for Fusion Applications",ORNL/TM-7828(1981).
15) ICRP Publication-51:"Data for Use in Protection Against External Radiation",(1987).

Table 1 Materials in HIL086R library

1	water	6	polyethylene
2	ordinary concrete	7	heavy concrete
3	iron	8	lead
4	air	9	aluminum
5	graphite	10	soil

Table 3 Upper energy boundaries of gamma-rays in units of MeV.

1	20.0	9	6.0	17	2.0
2	14.0	10	5.5	18	1.5
3	12.0	11	5.0	19	1.0
4	10.0	12	4.5	20	0.4
5	8.0	13	4.0	21	0.2
6	7.5	14	3.5	22	0.1
7	7.0	15	3.0		0.01
8	6.5	16	2.0		

Table 2 Group number vs. upper energy boundaries of neutrons in units of MeV.

1	400.	24	40.	47	0.907
2	375.	25	35.	48	0.743
3	350.	26	30.	49	0.498
4	325.	27	27.5	50	0.334
5	300.	28	25.	51	0.224
6	275.	29	22.5	52	0.150
7	250.	30	19.6	53	8.65E-2
8	225.	31	17.5	54	3.18E-2
9	200.	32	14.9	55	1.50E-2
10	180.	33	13.5	56	7.10E-3
11	160.	34	12.2	57	3.35E-3
12	140.	35	10.0	58	1.58E-3
13	120.	36	8.19	59	4.54E-4
14	110.	37	6.70	60	1.01E-4
15	100.	38	5.49	61	2.26E-5
16	90.	39	4.49	62	1.07E-5
17	80.	40	3.68	63	5.04E-6
18	70.	41	3.01	64	2.38E-6
19	65.	42	2.46	65	1.12E-6
20	60.	43	2.02	66	4.14E-7
21	55.	44	1.65		1.00E-10
22	50.	45	1.35		
23	45.	46	1.11		

Table 4 Atomic number densities

unit($10^{24}/cm^3$)

	Water	Graphite	Polyethylene	Air	Lead
H	6.6738-2¥)		7.9793-2		
C		8.5240-2	3.9930-2		
N				3.9099-5	
O	3.3369-2			1.0538-5	
Pb					3.2960-2

unit($10^{24}/cm^3$)

	Aluminium	Iron	Ordinary concrete**)	Heavy-Concrete	Soil ***)
H			1.3851-2	9.9885-3	6.6300-3
C			1.1542-4		
O			4.5921-2	4.3899-2	2.0200-2
Mg			1.2388-4	4.3265-5	
Al	6.0244-2		1.7409-3	1.6502-4	1.7500-3
Si			1.6621-2	3.7264-2	5.7000-3
K			4.6205-4		3.8600-4
Ca			1.5025-3	2.2782-3	5.2000-4
Fe		8.4869-2	3.4510-4	2.3602-2	5.2100-4

*) JAERI-M 6928(1977),
**) 02a-concrete, ANL-5800 p.660,
***) Compendium II p.358
¥) read as 6.6738×10^{-2}

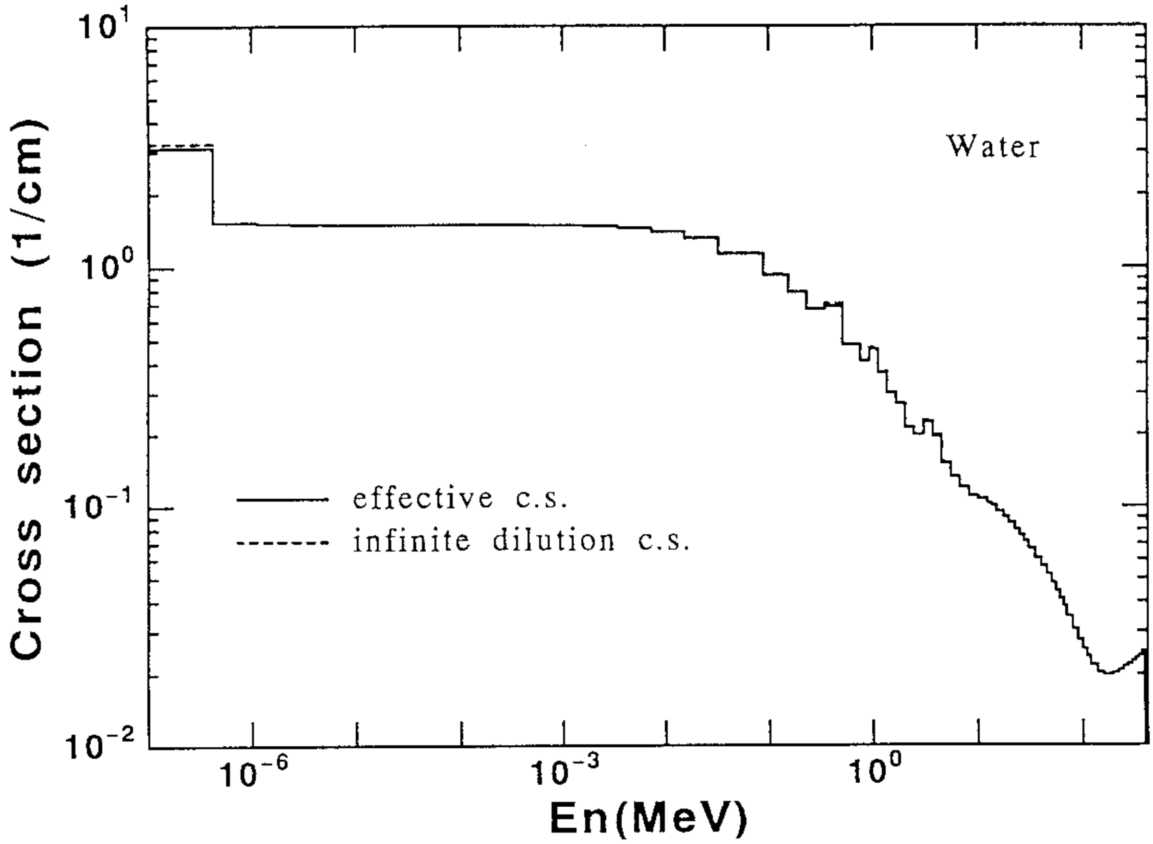

Fig. 1 Comparison between effective and infinite dilution total cross sections of water in HILO86R library.

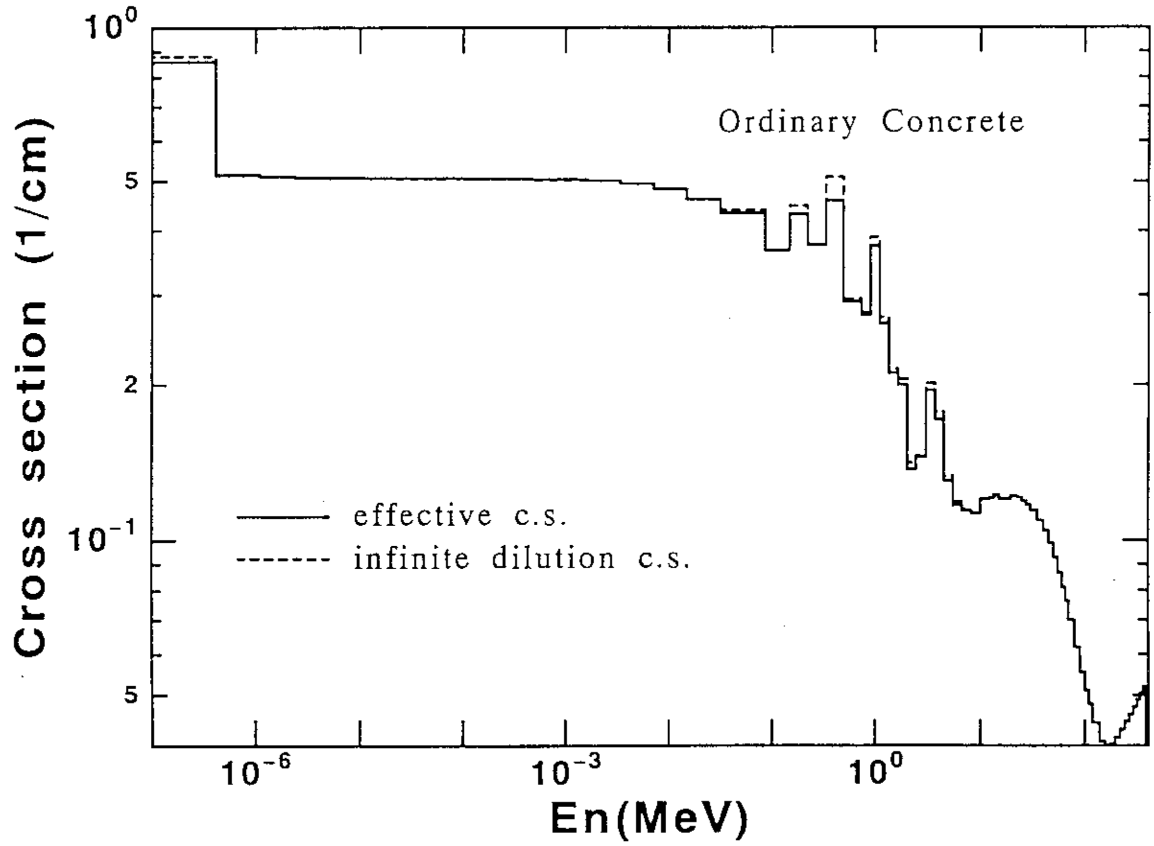

Fig.2 Comparison between effective and infinite dilution total cross sections of ordinary concrete in HILO86R library.

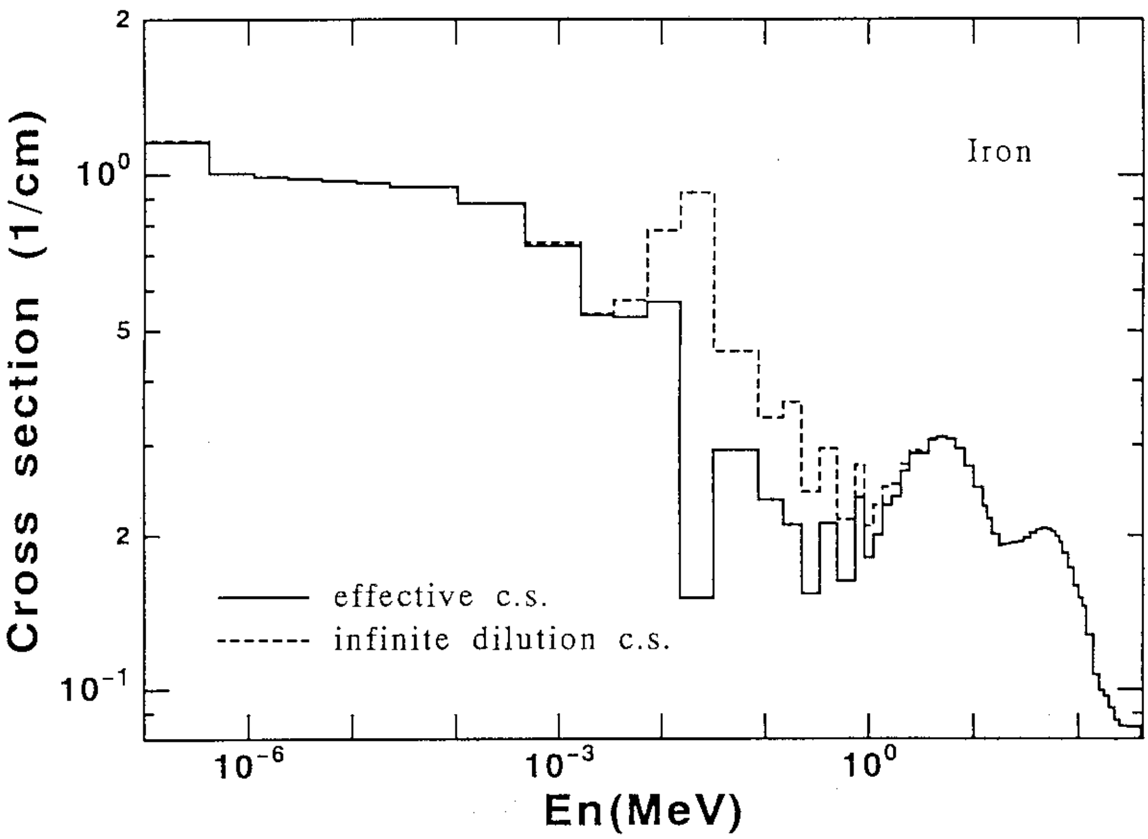

Fig. 3 Comparison between effective and infinite dilution total cross sections of iron in HILO86R library.

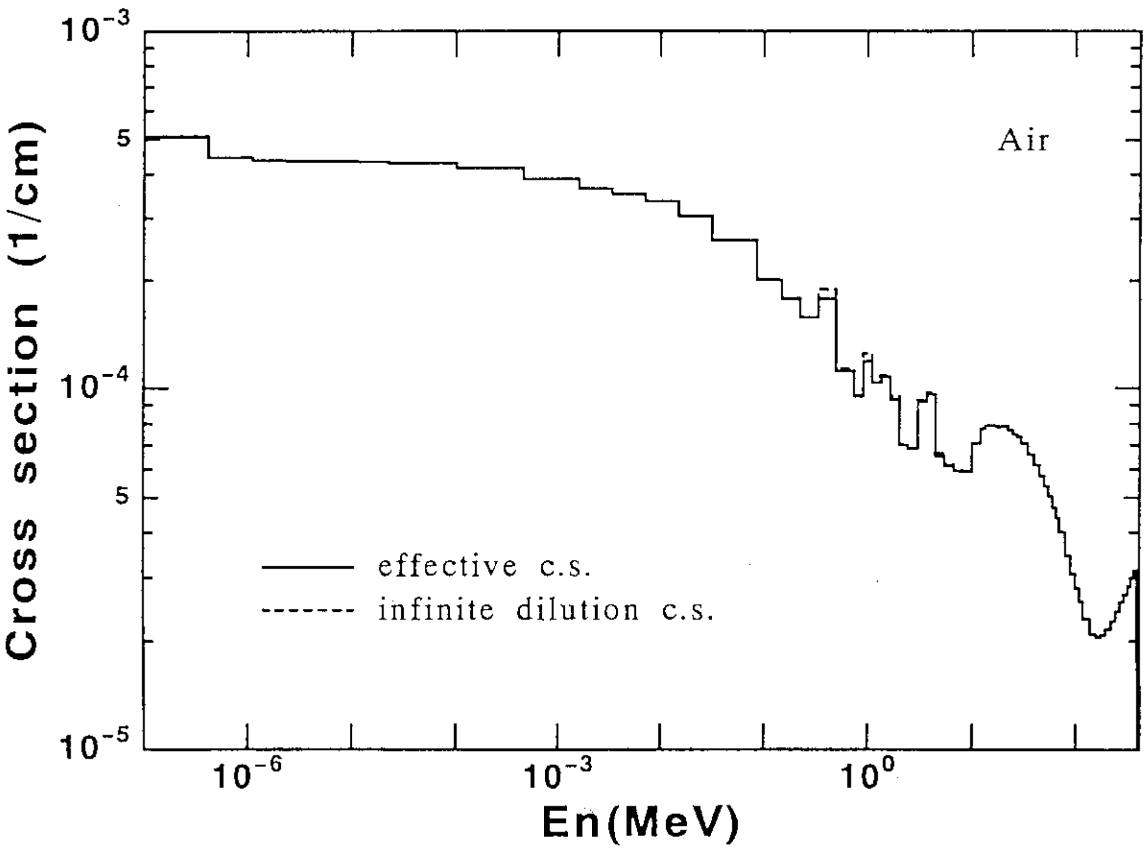

Fig. 4 Comparison between effective and infinite dilution total cross sections of air in HILO86R library.

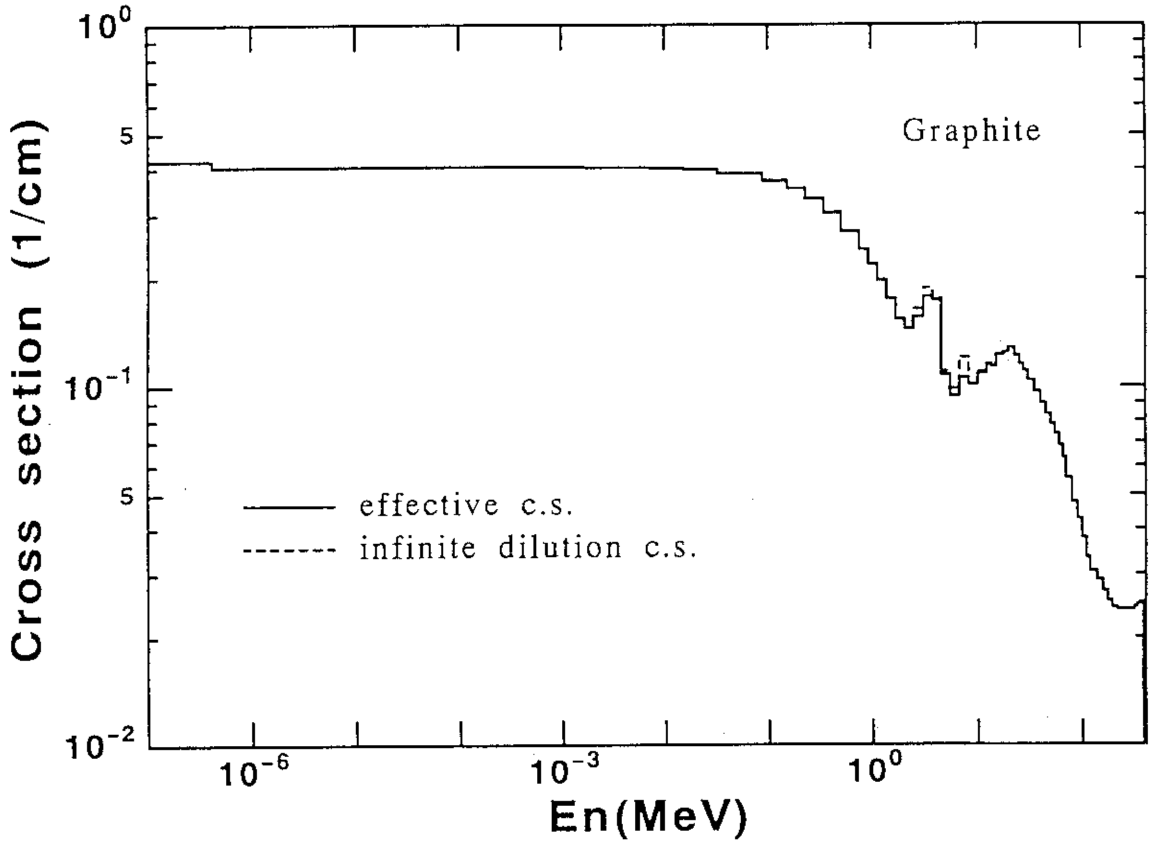

Fig. 5 Comparison between effective and infinite dilution total cross sections of graphite in HILO86R library.

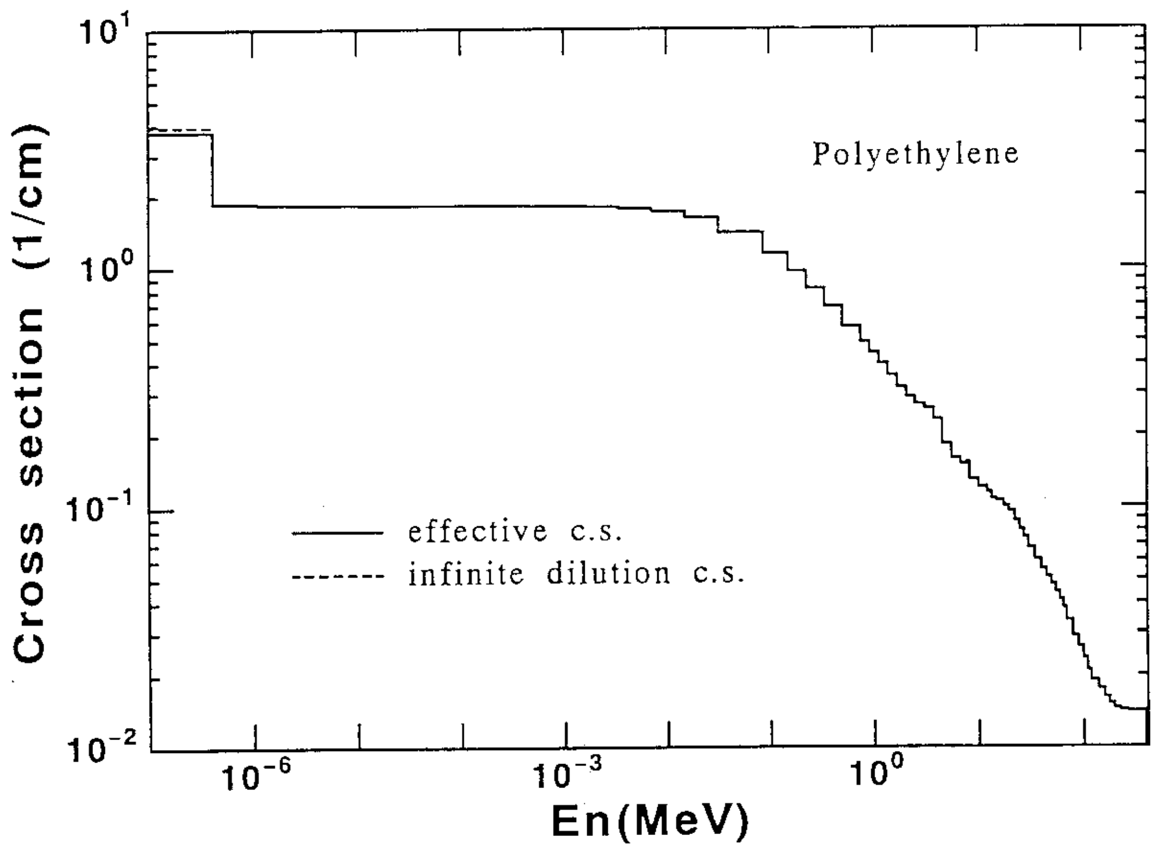

Fig. 6 Comparison between effective and infinite dilution total cross sections of polyethylene in HILO86R library.

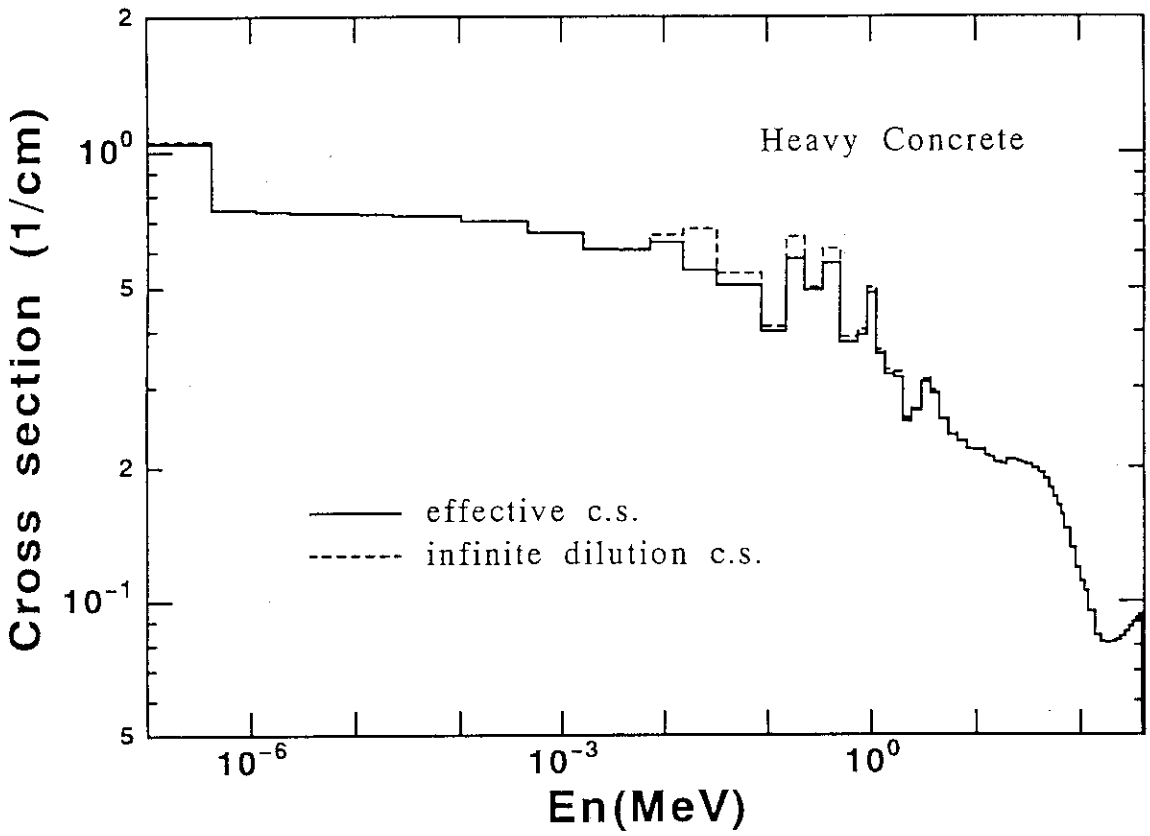

Fig.7 Comparison between effective and infinite dilution total cross sections of heavy concrete in HILO86R library.

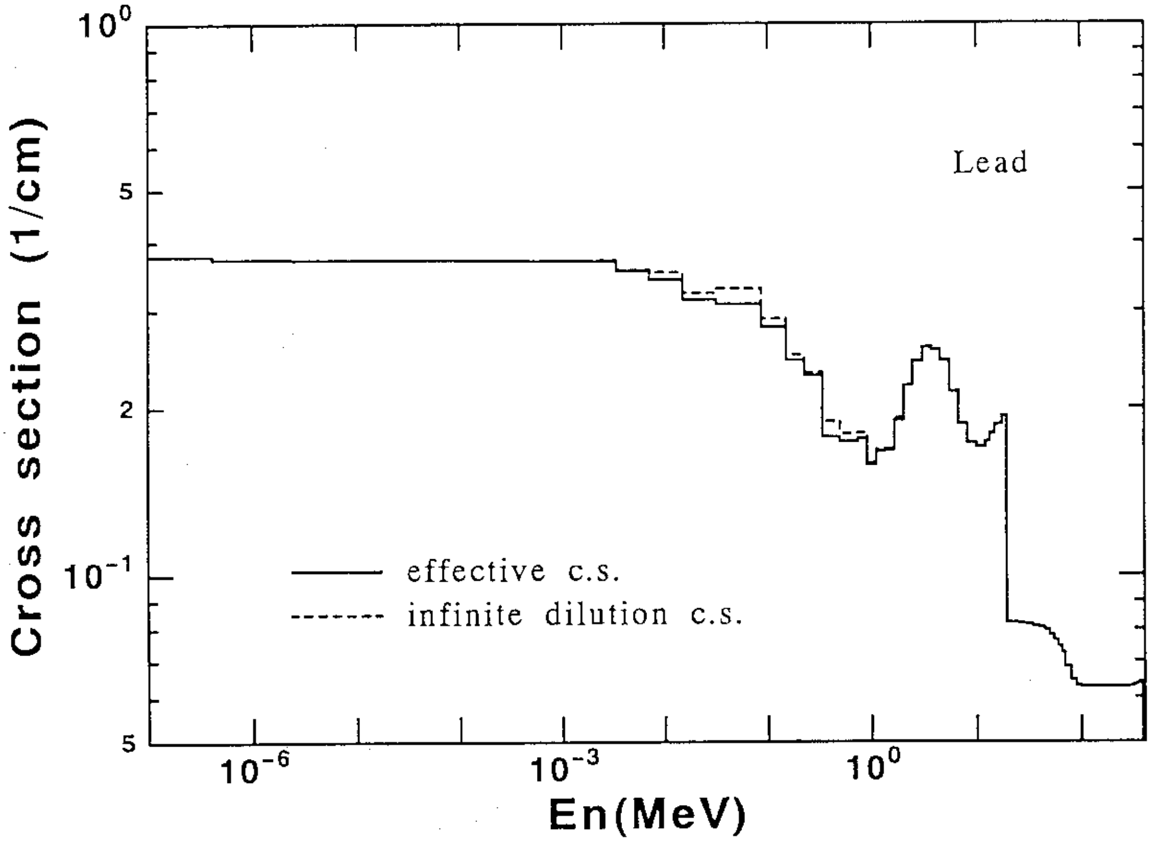

Fig.8 Comparison between effective and infinite dilution total cross sections of lead in HILO86R library.

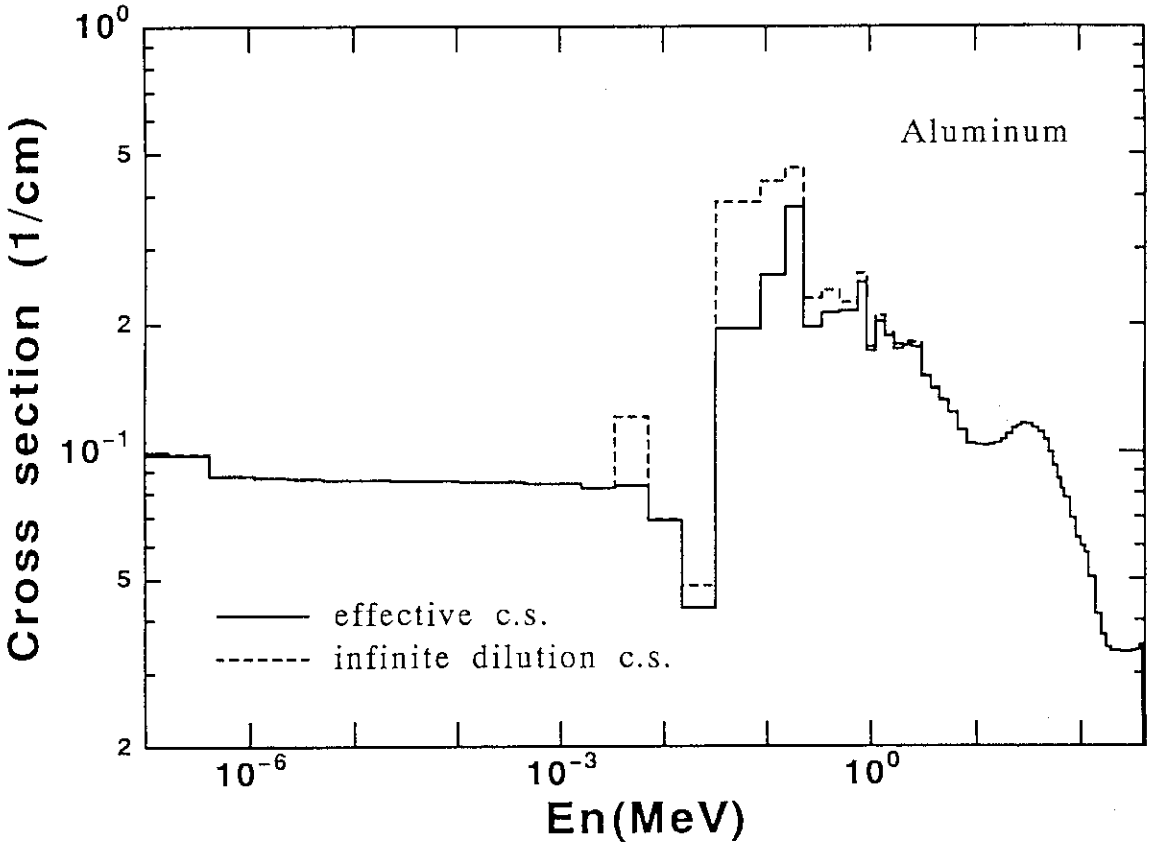

Fig. 9 Comparison between effective and infinite dilution total cross sections of aluminium in HILO86R library.

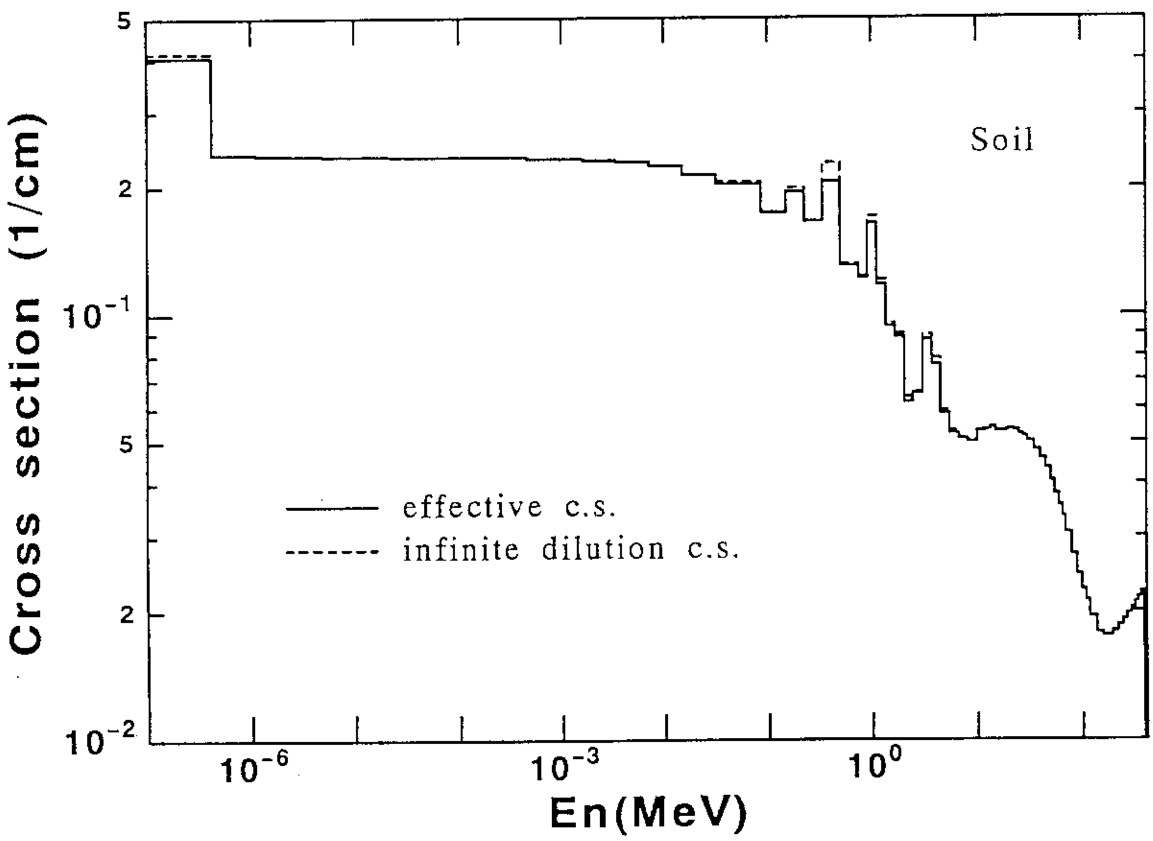

Fig.10 Comparison between effective and infinite dilution total cross sections of soil in HILO86R library.

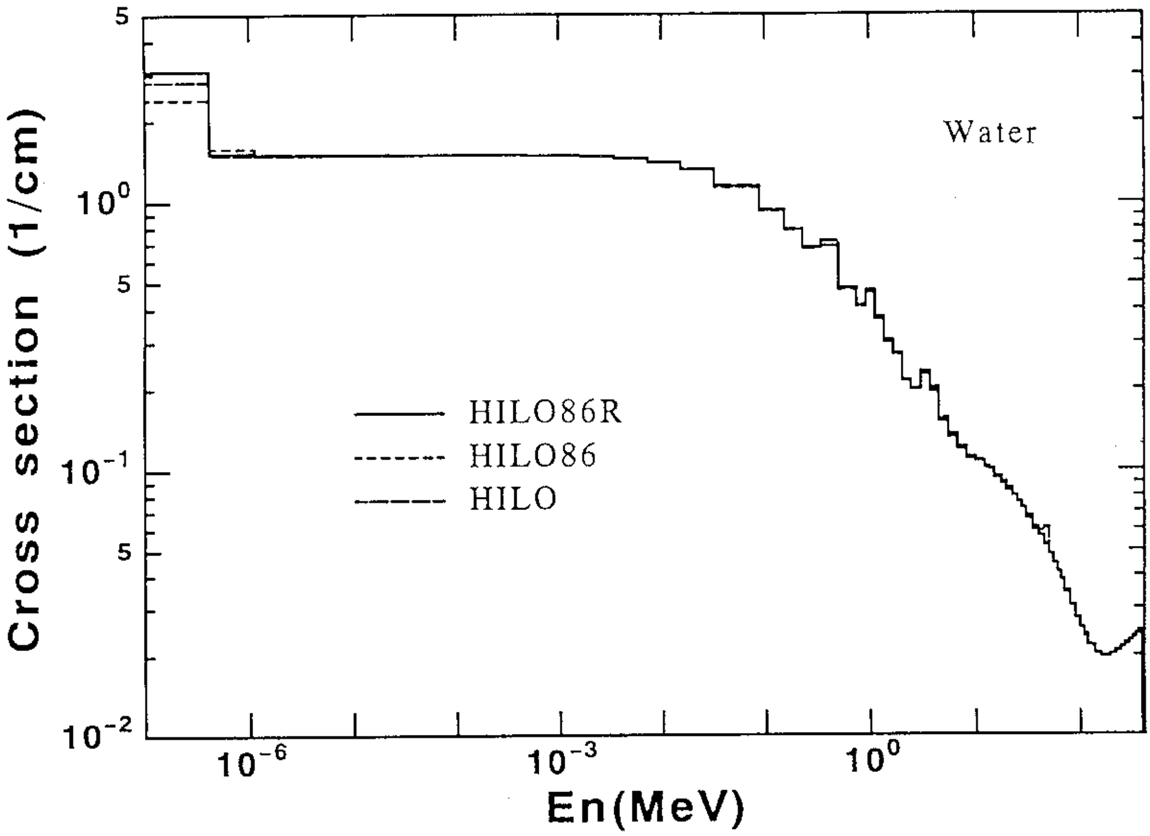

Fig.11 Comparison of total cross sections of water in HILO86R, HILO86 and HILO libraries.

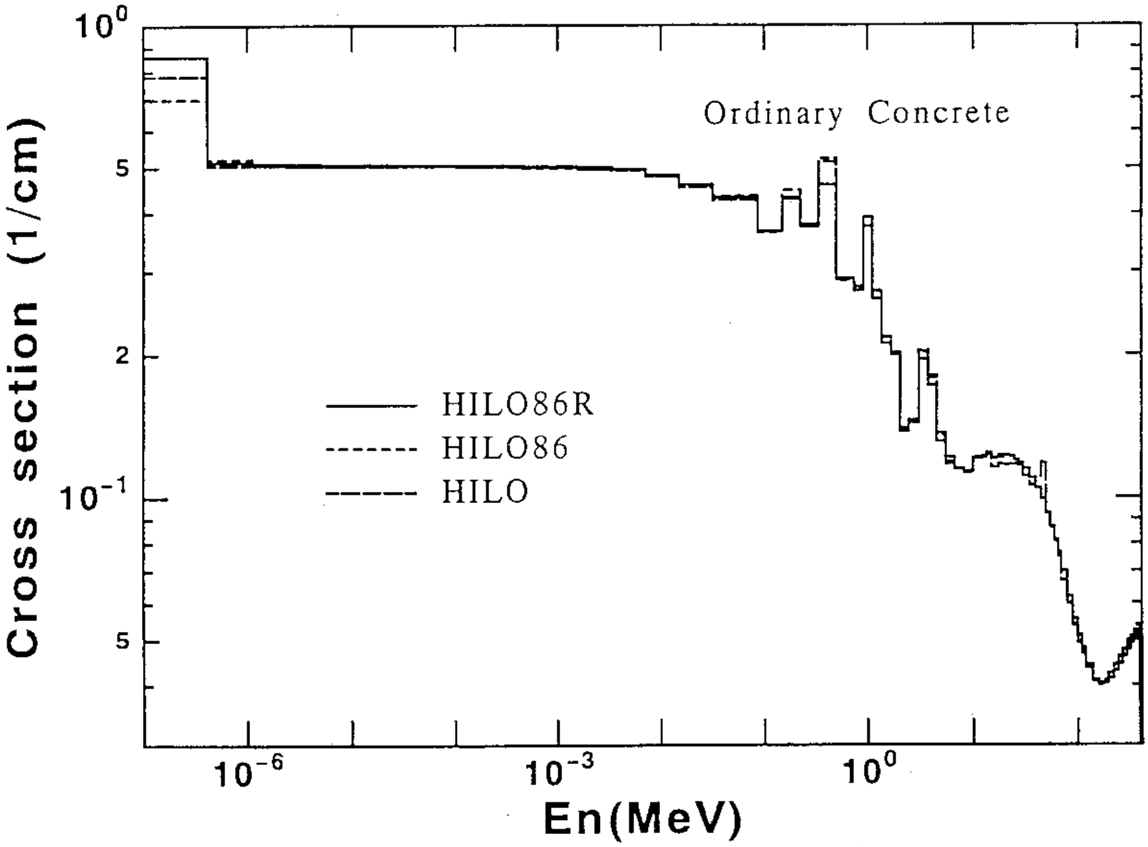

Fig.12 Comparison of total cross sections of ordinary concrete in HILO86R, HILO86 and HILO libraries.

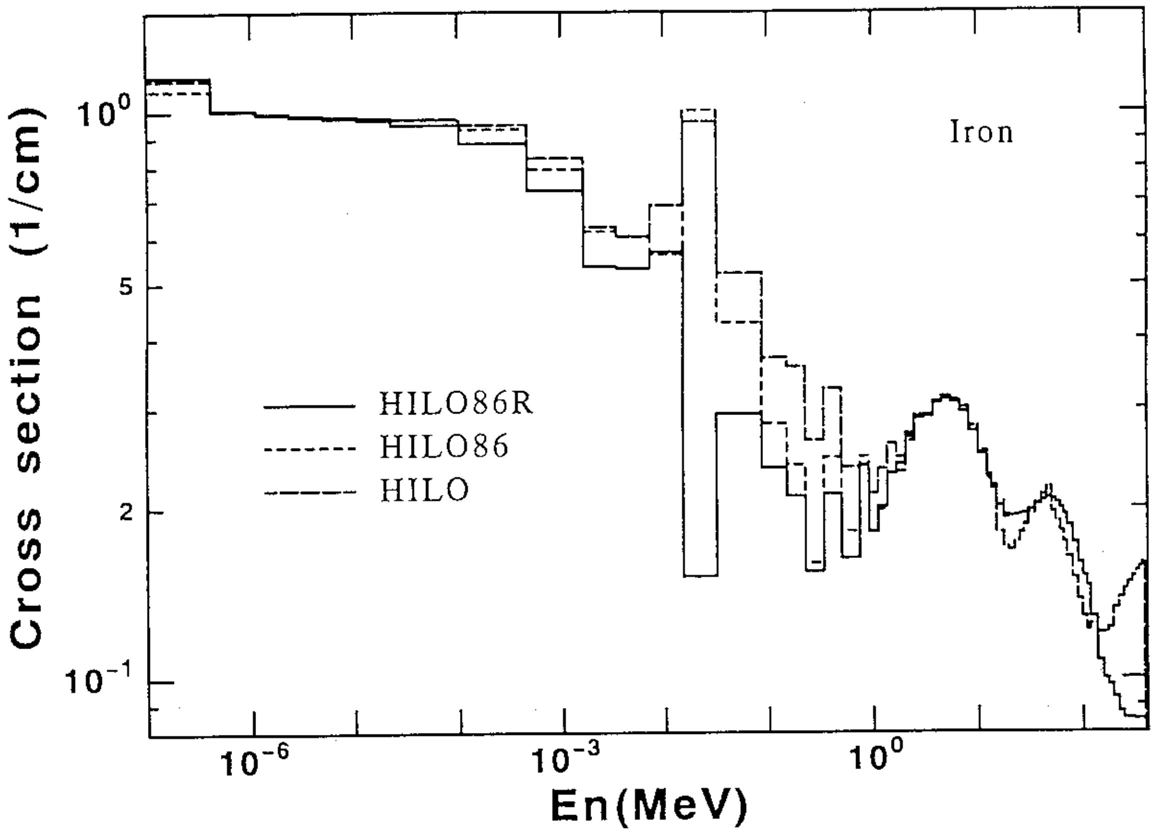

Fig.13 Comparison of total cross sections of iron in HILO86R, HILO86 and HILO libraries.

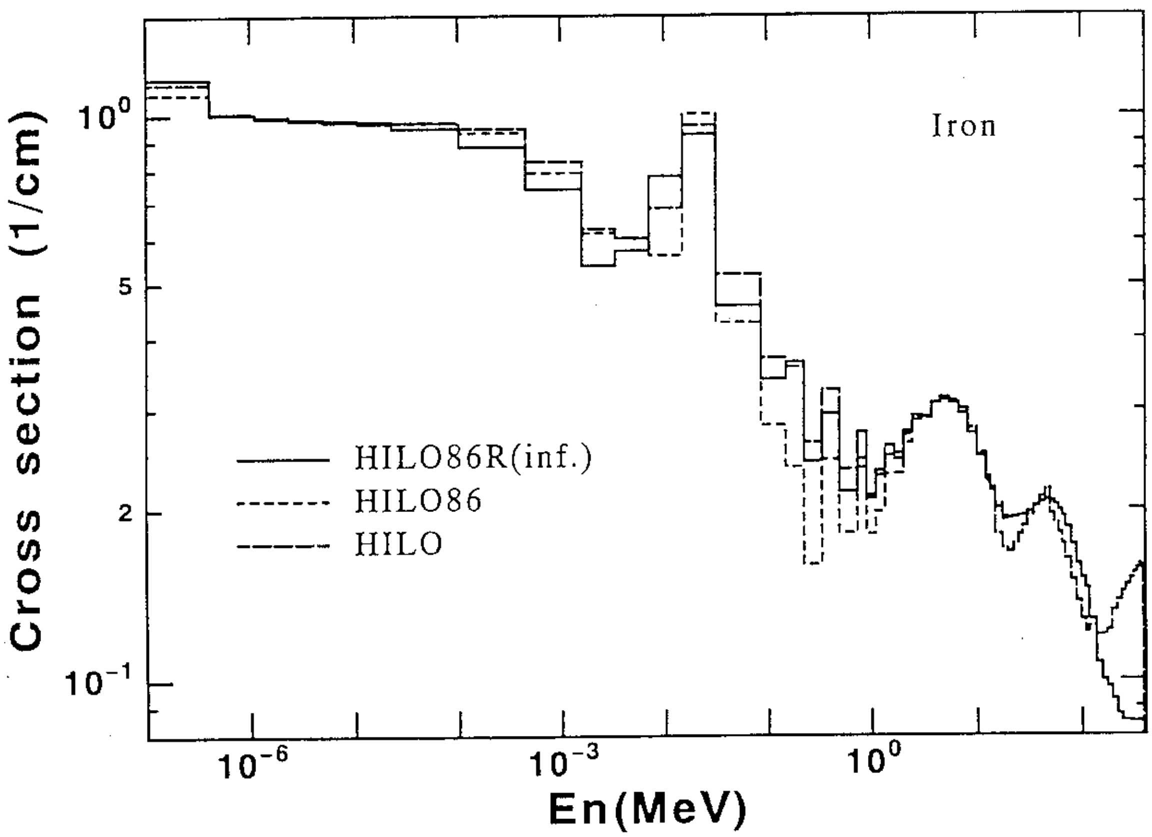

Fig.14 Comparison of total cross sections in HILO86 and HILO with infinite dilution total cross section of HILO86R library.

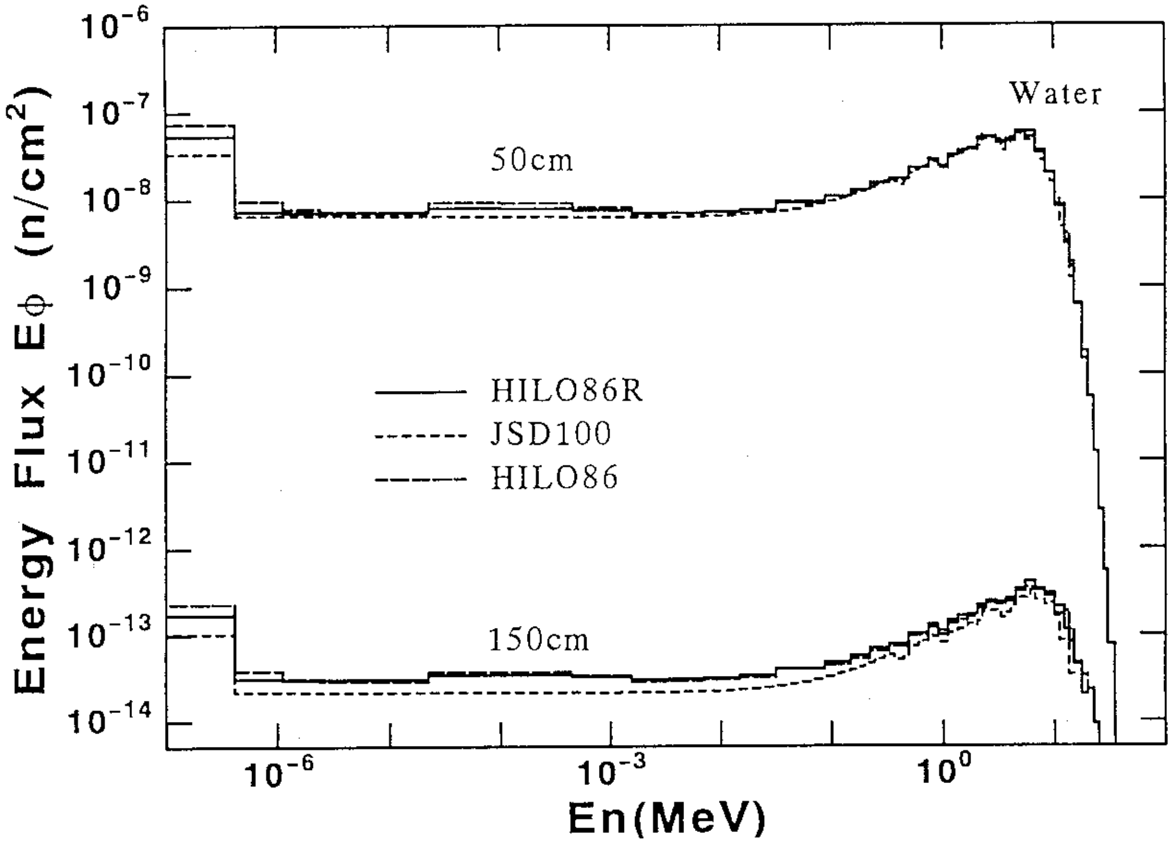

Fig.15 Energy spectra at thicknesses of 50 and 150cm in water for ^{252}Cf neutron source.

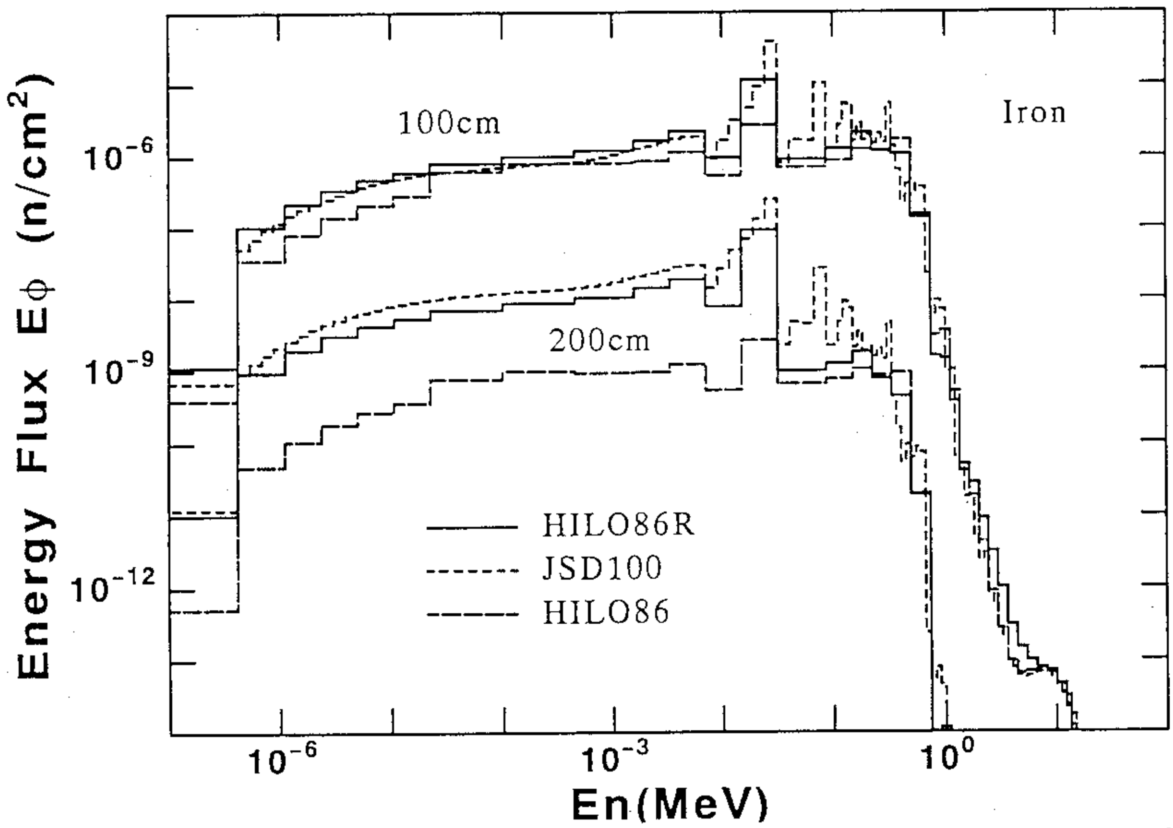

Fig.16 Energy spectra at thicknesses of 100 and 200cm in iron for ^{252}Cf neutron source.

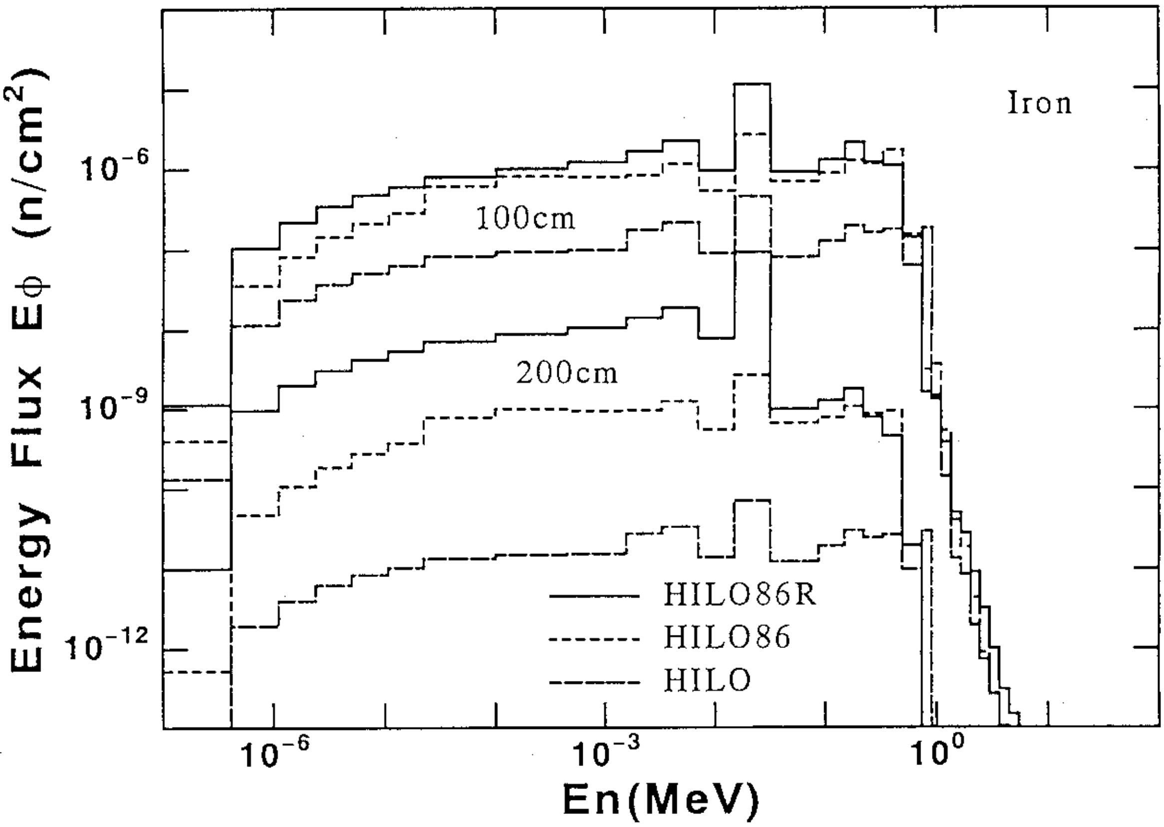

Fig. 17 Energy spectra at thicknesses of 100 and 200 cm in iron for ^{252}Cf neutron source.

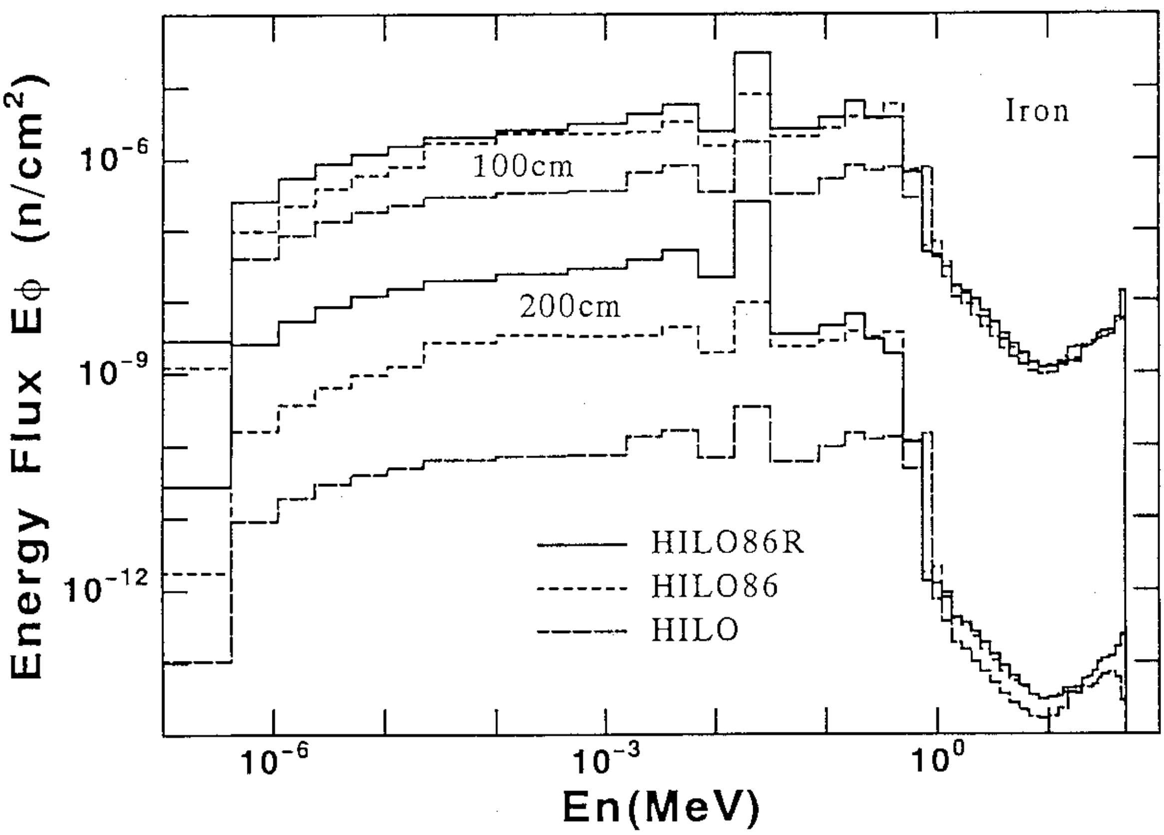

Fig. 18 Energy spectra at thicknesses of 100 and 200 cm in iron for 50 MeV neutron source.

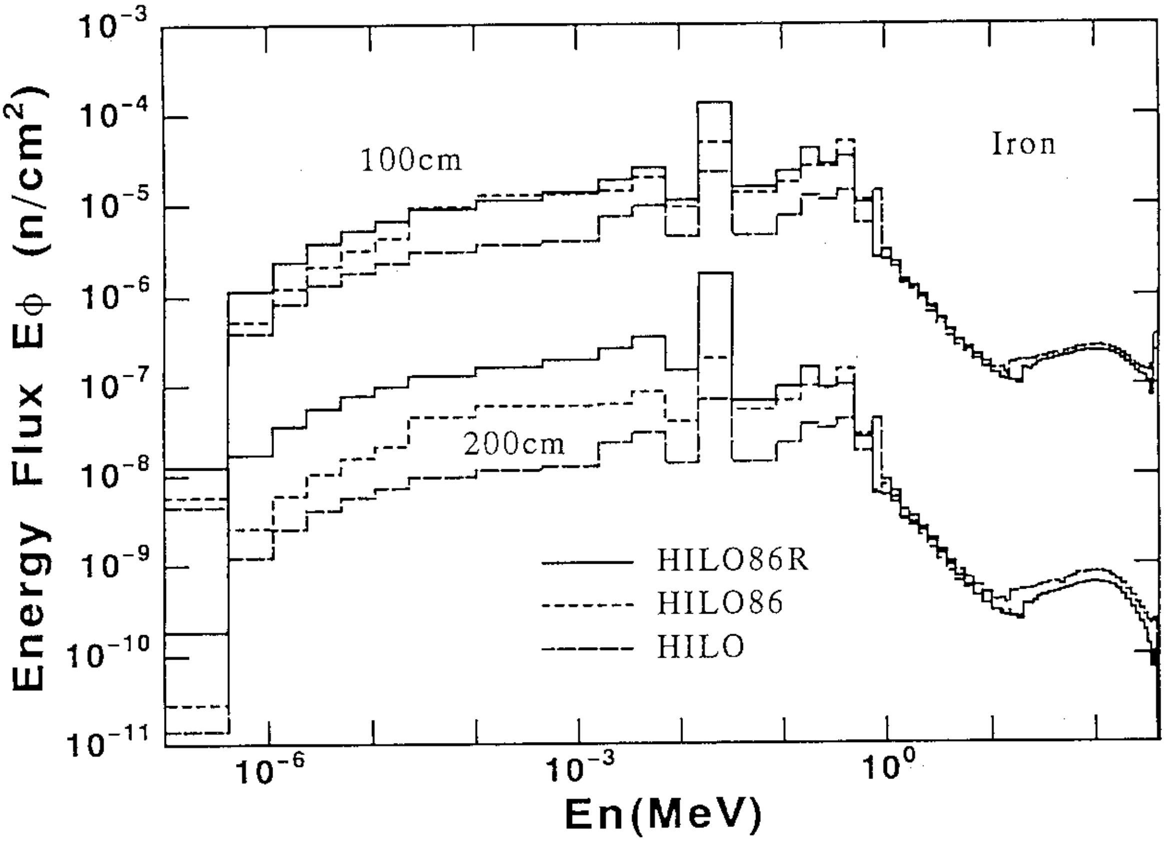

Fig.19 Energy spectra at thicknesses of 100 and 200cm in iron for 400MeV neutron source.

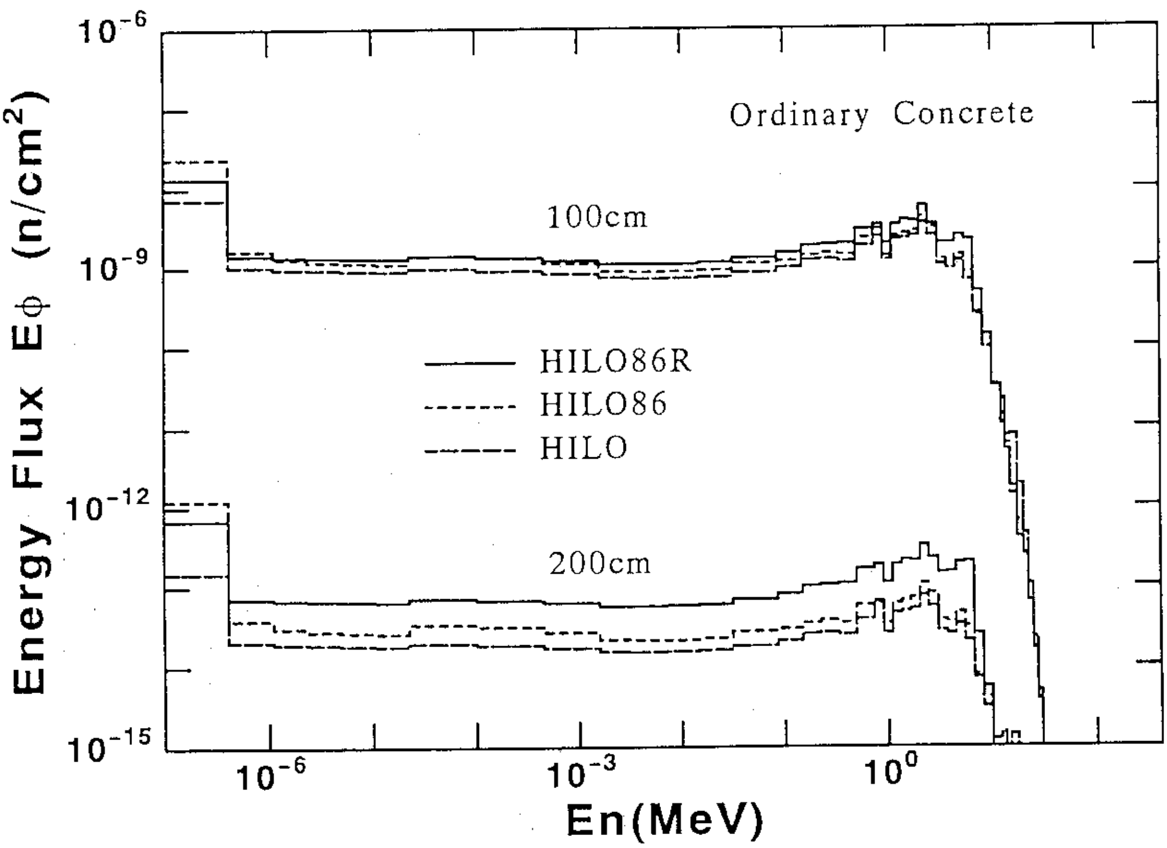

Fig.20 Energy spectra at thicknesses of 100 and 200cm in ordinary concrete for ^{252}Cf neutron source.

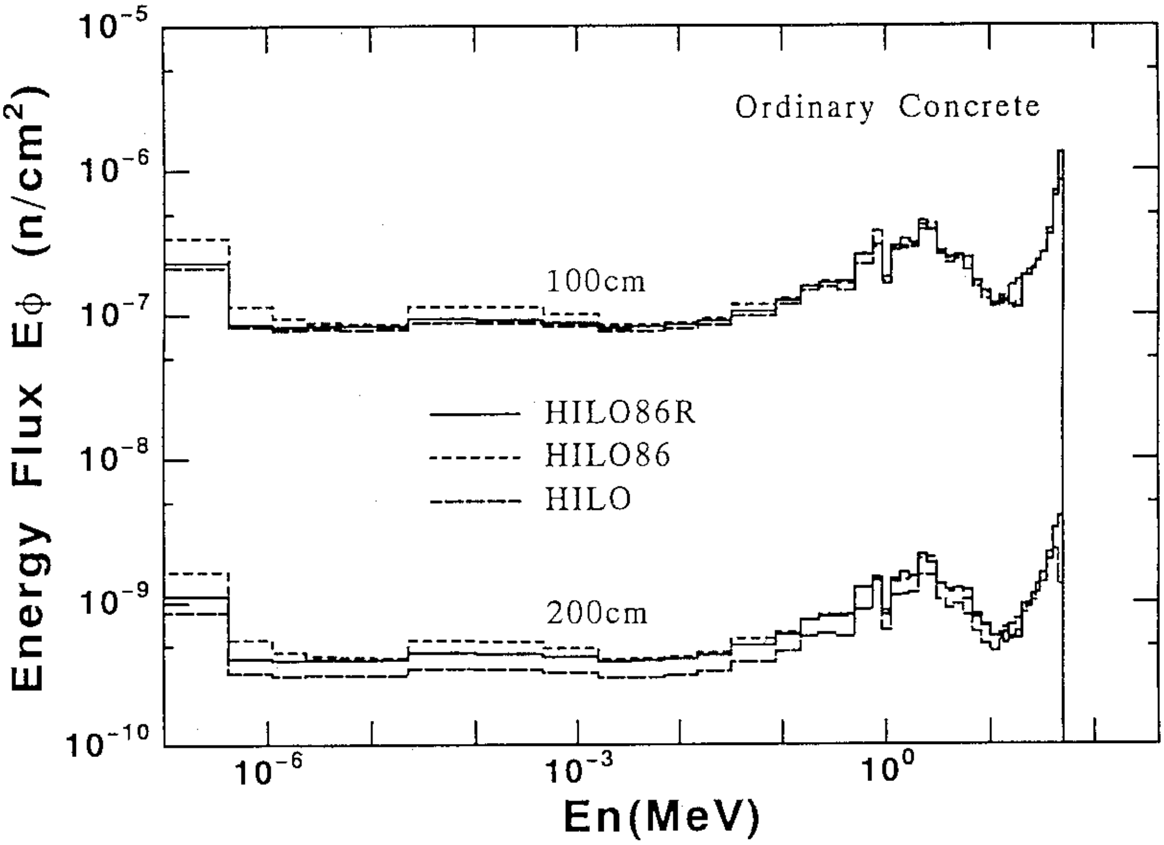

Fig. 21 Energy spectra at thicknesses of 100 and 200 cm in ordinary concrete for 50 MeV neutron source.

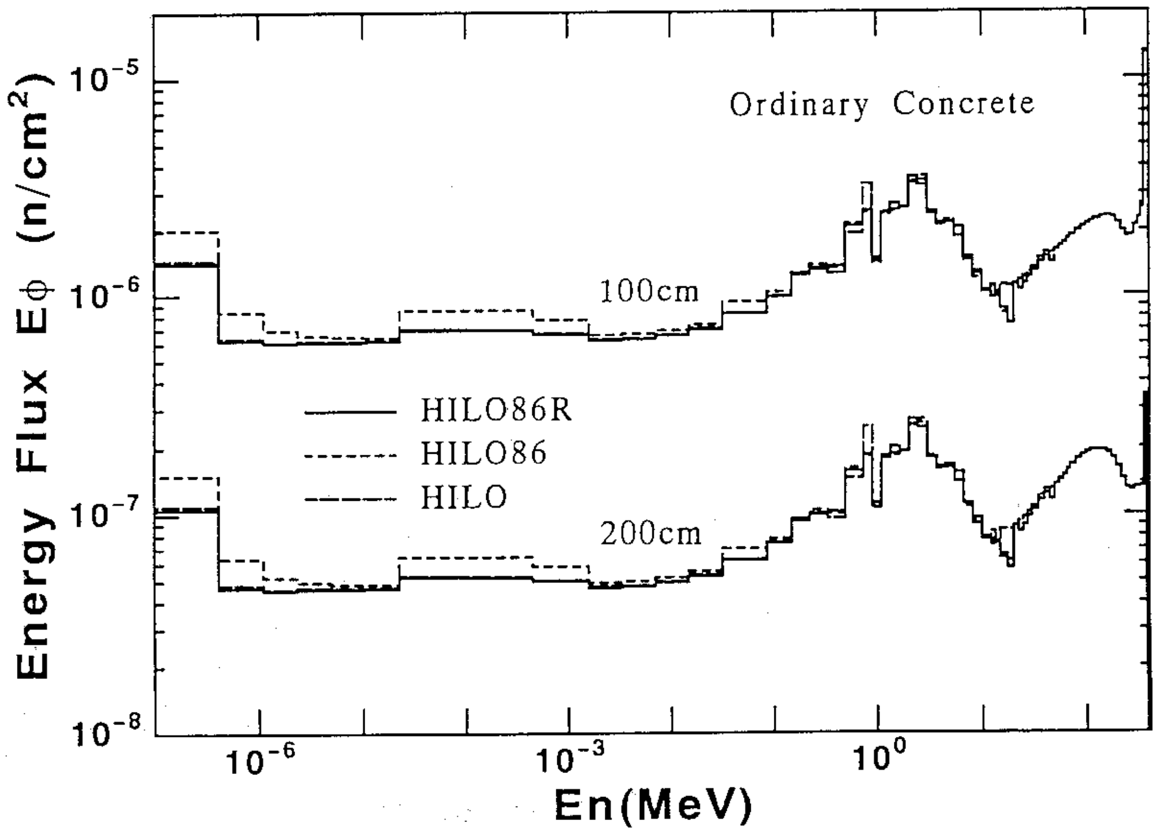

Fig. 22 Energy spectra at thicknesses of 100 and 200 cm in ordinary concrete for 400 MeV neutron source.

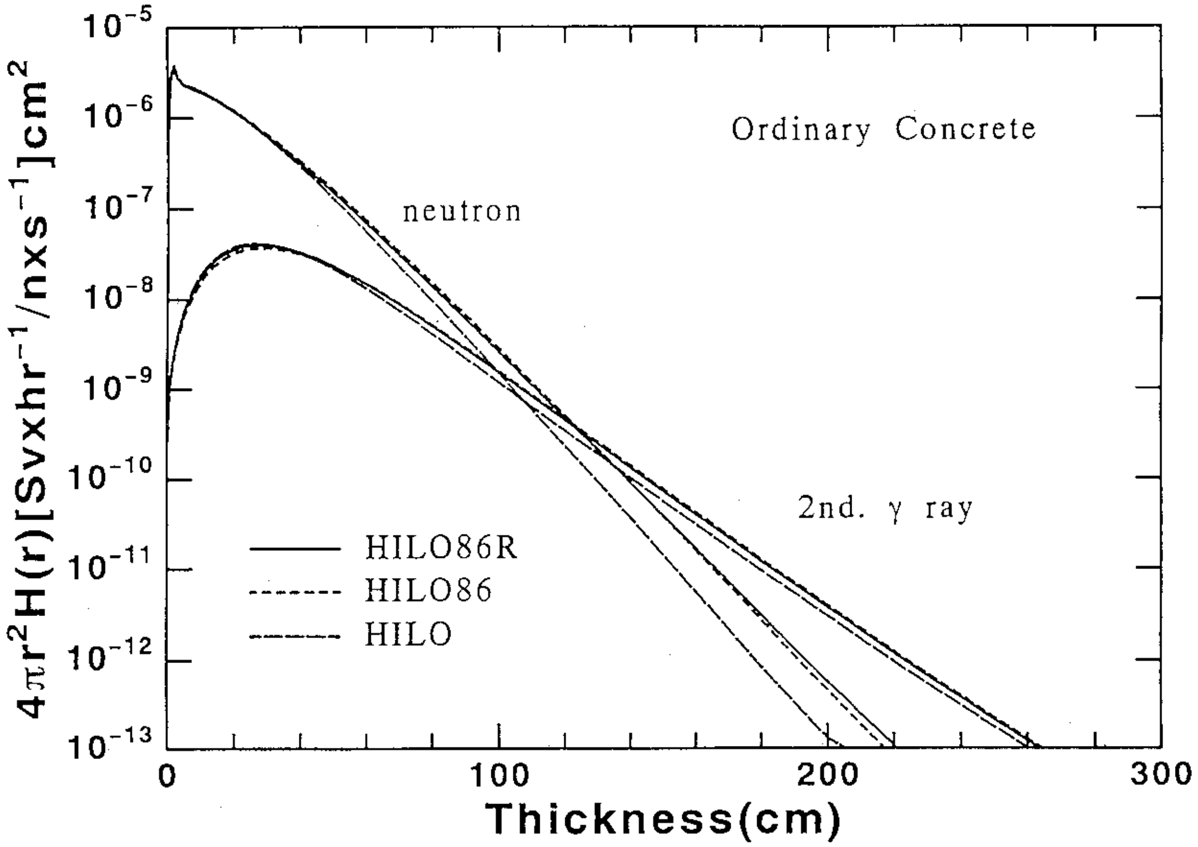

Fig.23 Attenuation of dose equivalent in ordinary concrete for ^{252}Cf neutron source.

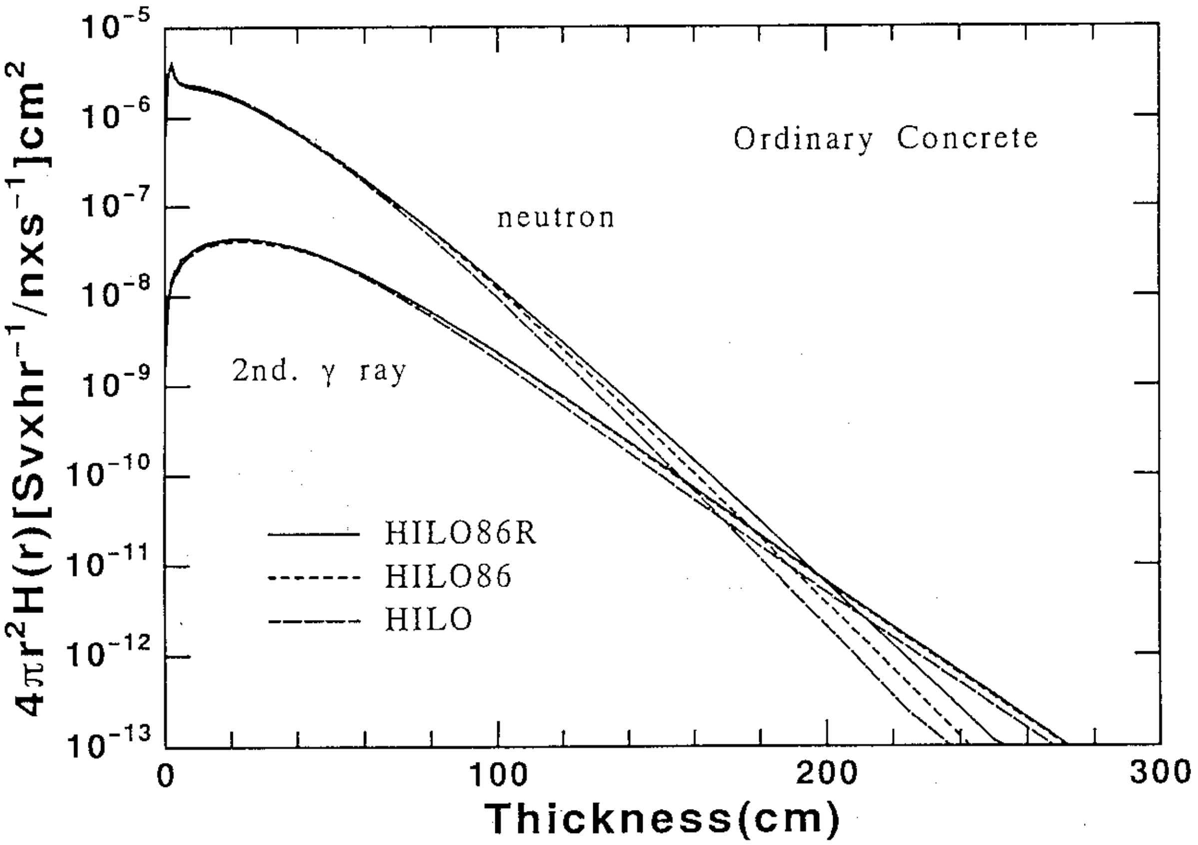

Fig.24 Attenuation of dose equivalent in ordinary concrete for 10 MeV neutron source.

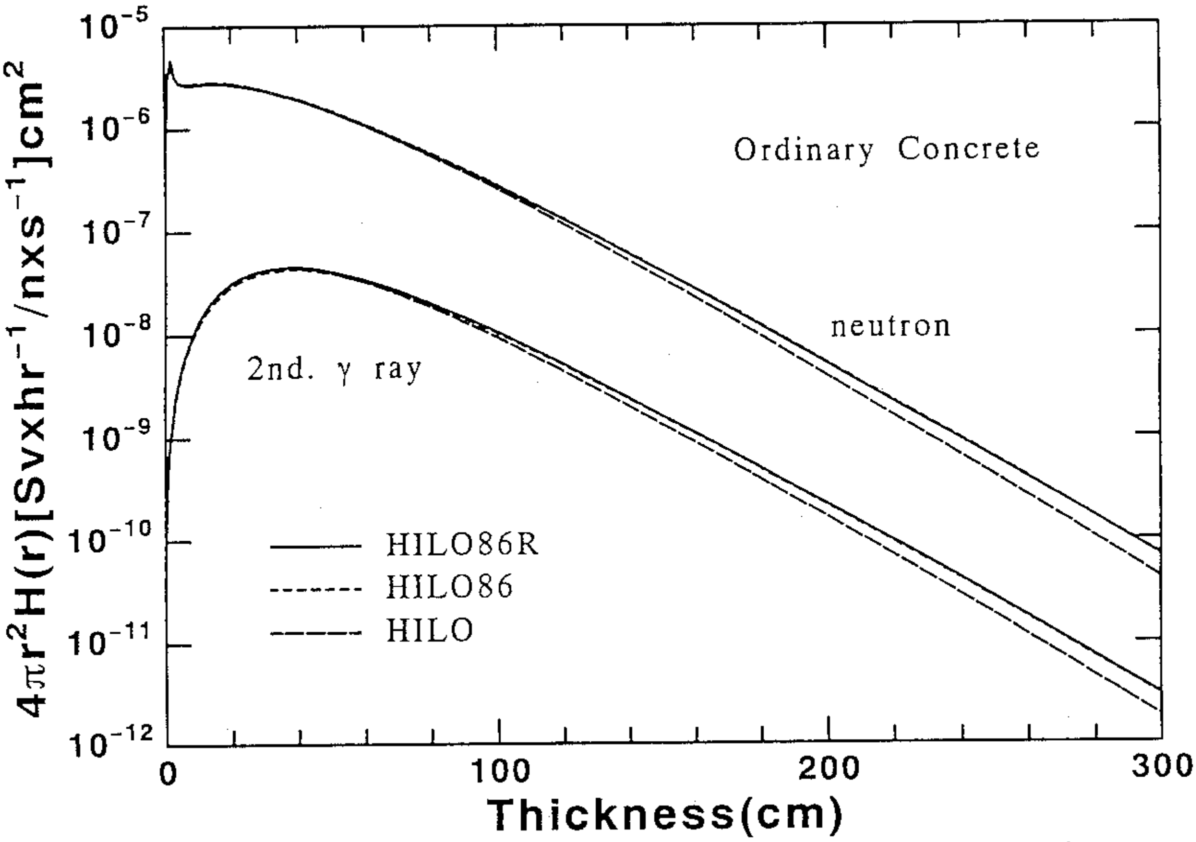

Fig.25 Attenuation of dose equivalent in ordinary concrete for 50MeV neutron source.

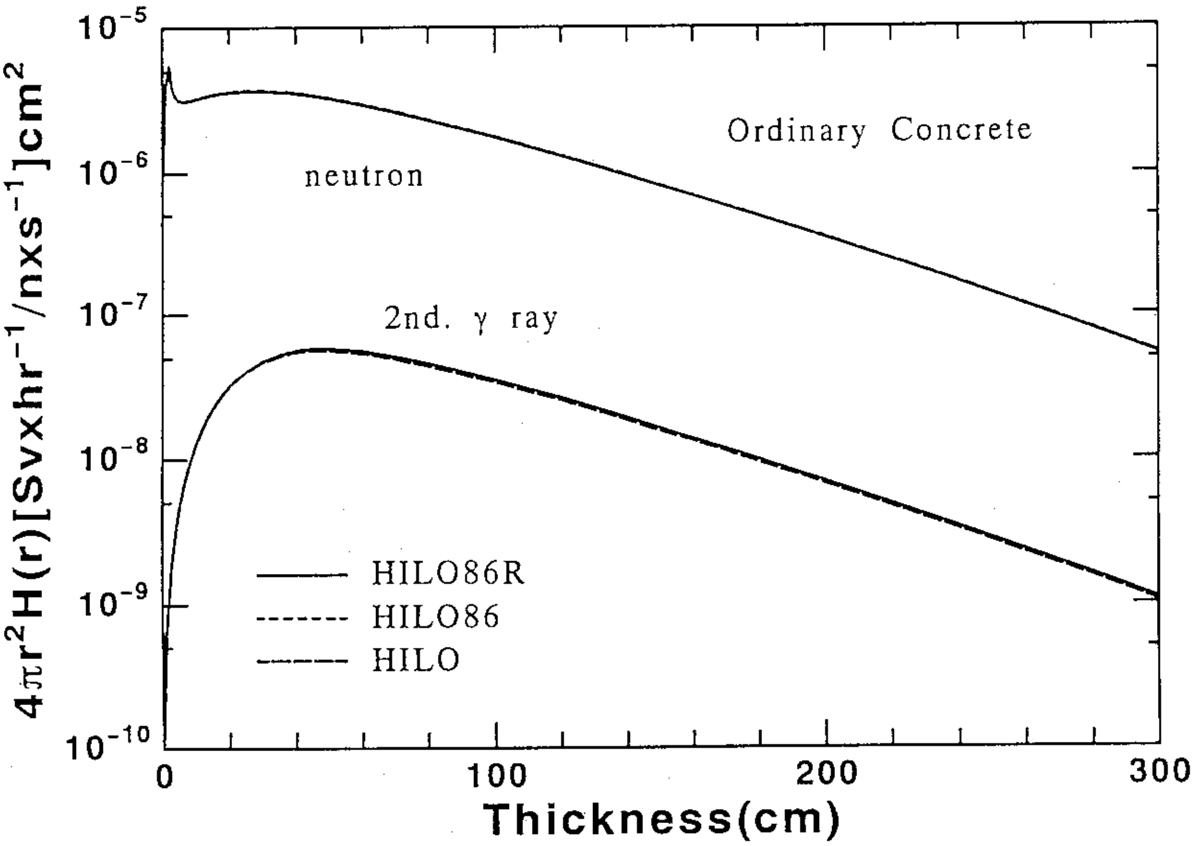

Fig.26 Attenuation of dose equivalents in ordinary concrete for 200MeV neutron source.

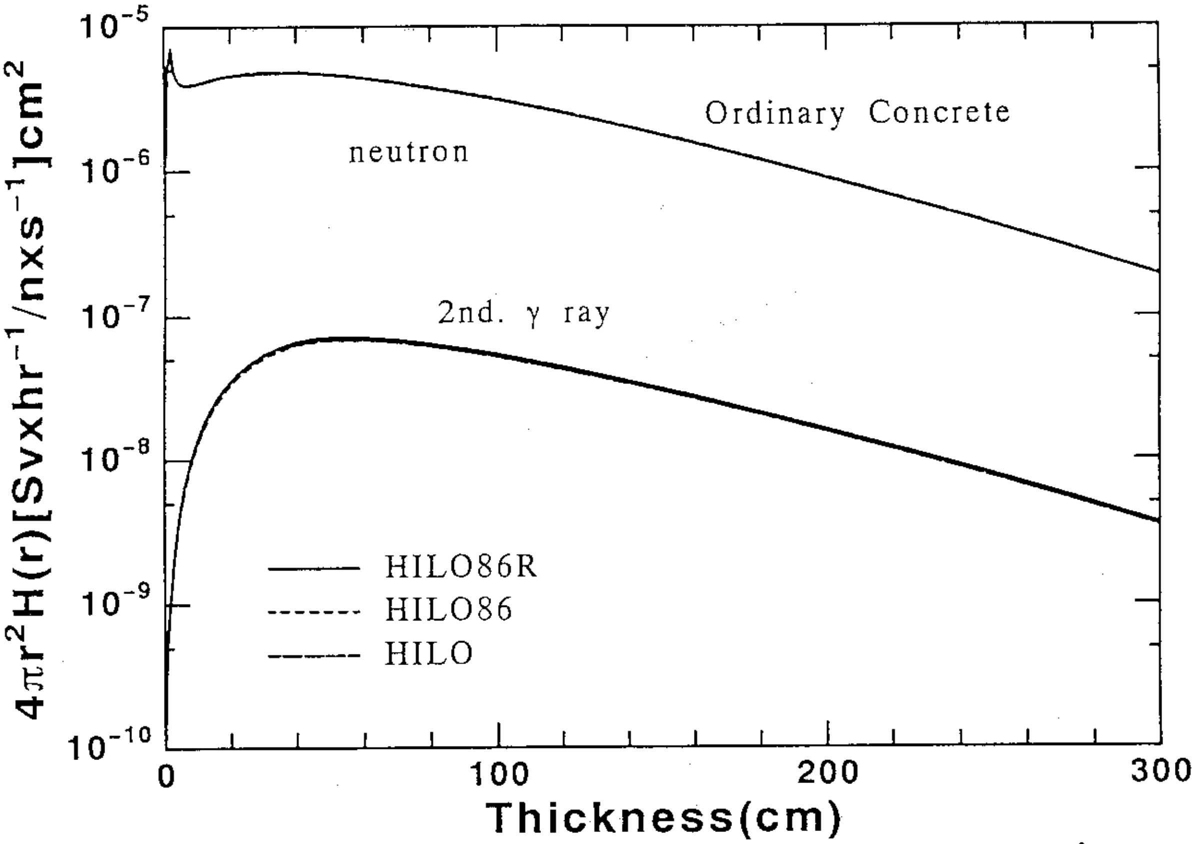

Fig.27 Attenuation of dose equivalents in ordinary concrete for 400MeV neutron source.

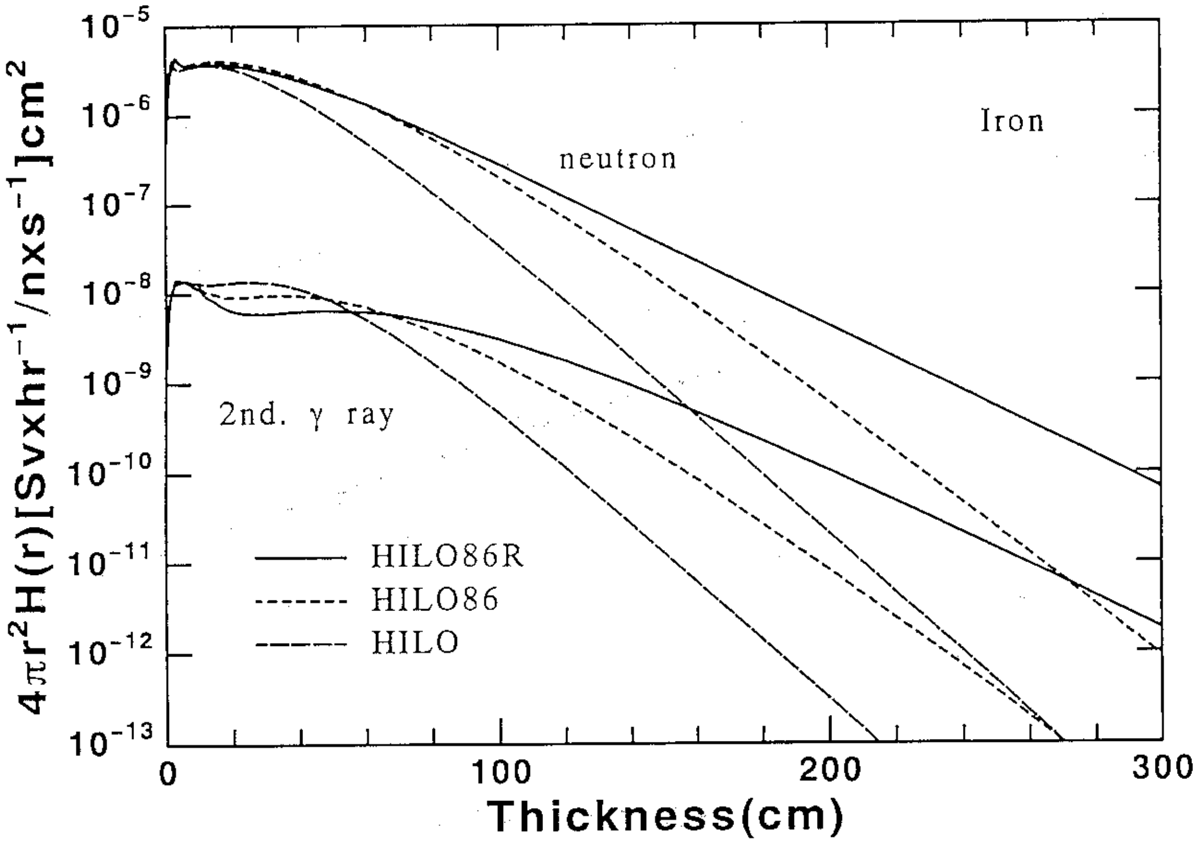

Fig.28 Attenuation of dose equivalent in iron for ^{252}Cf neutron source.

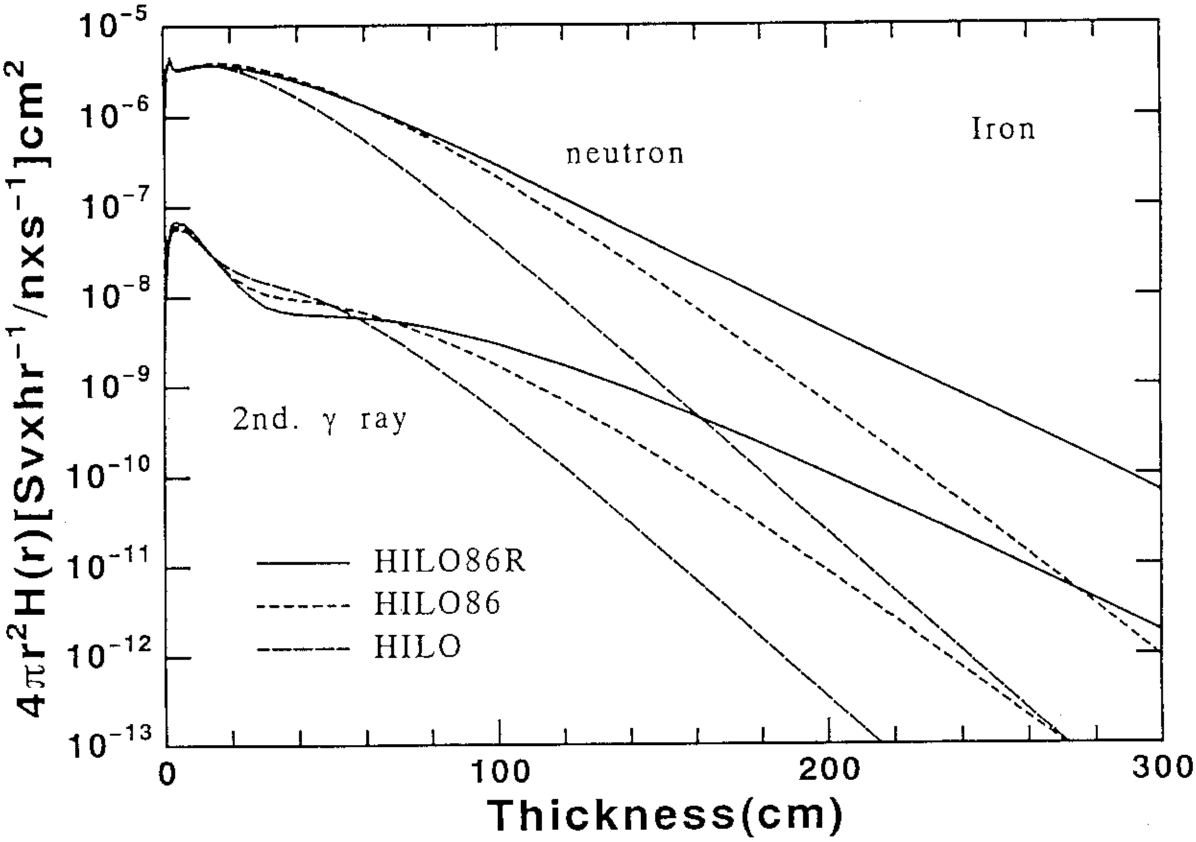

Fig.29 Attenuation of dose equivalent in iron for 10MeV neutron source.

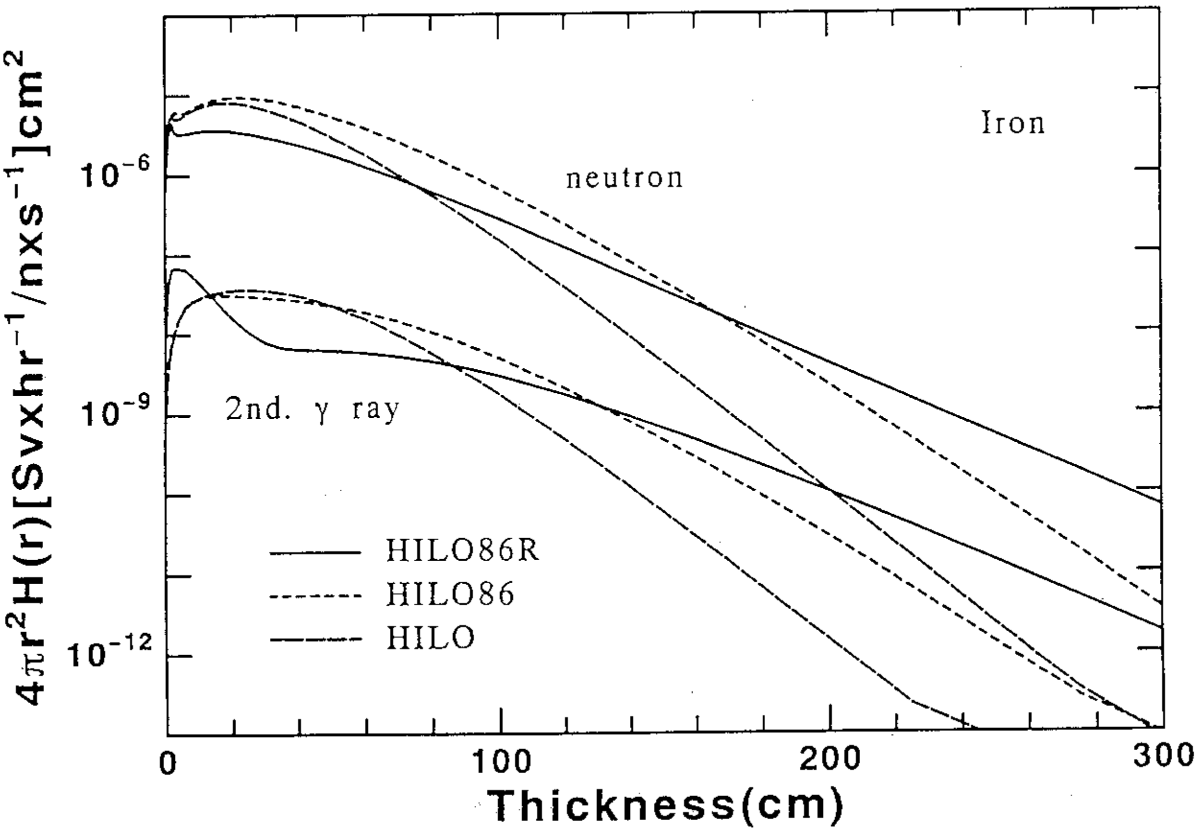

Fig.30 Attenuation of dose equivalent in iron for 50MeV neutron source.

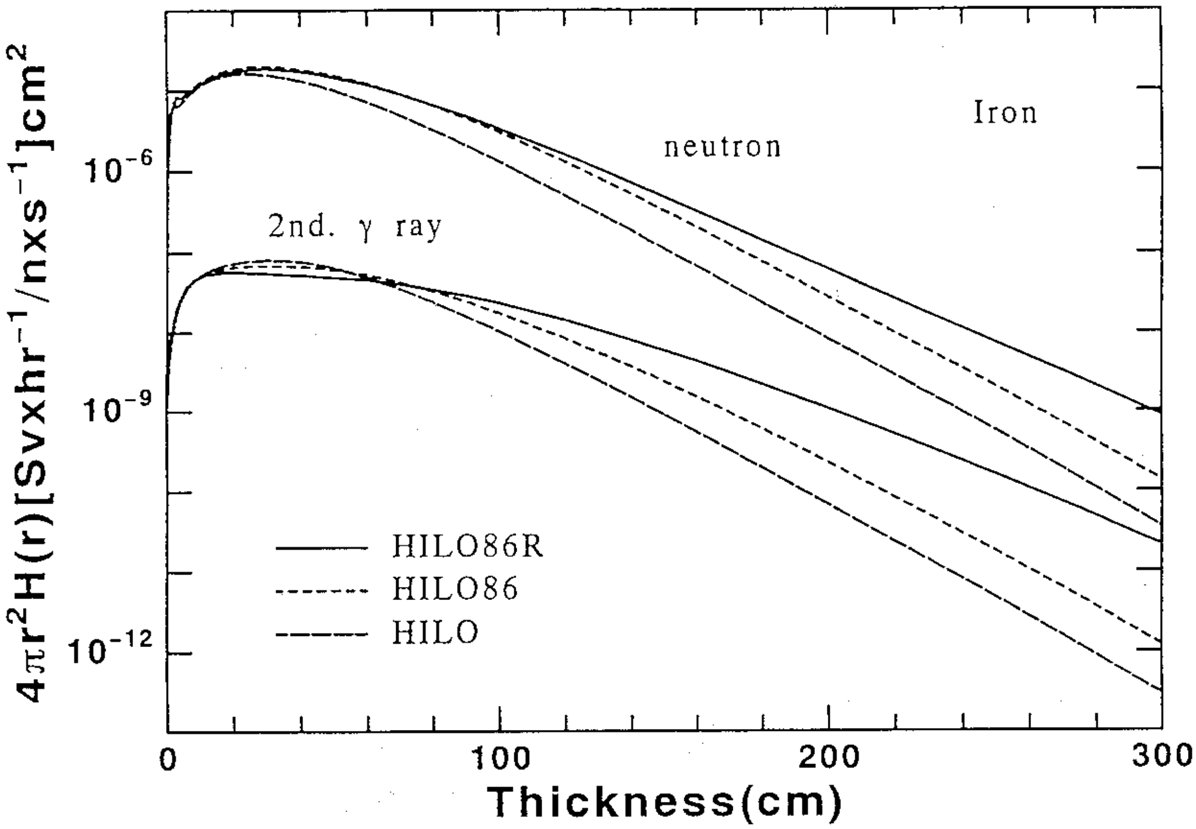

Fig. 31 Attenuation of dose equivalent in iron for 200MeV neutron source.

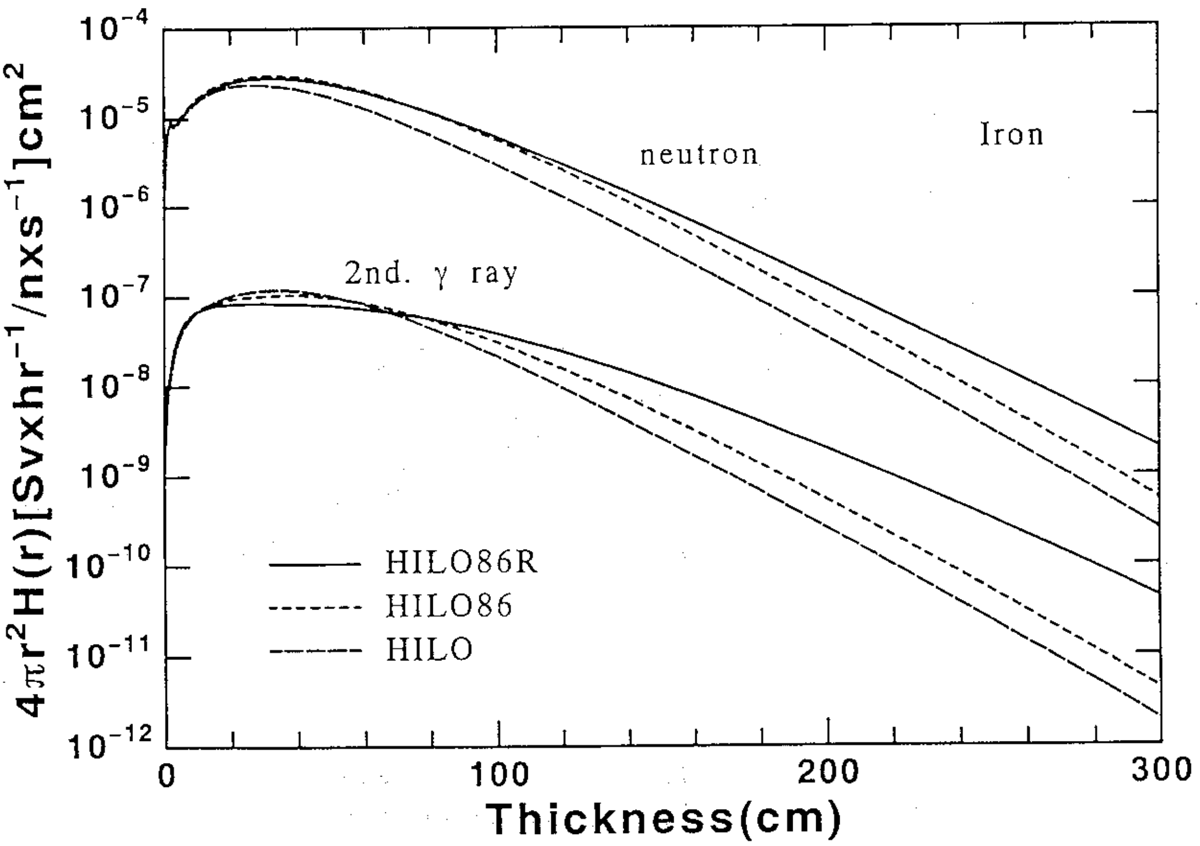

Fig. 32 Attenuation of dose equivalent in iron for 400MeV neutron source.

Appendix : HIL086R library

Contents

No.	File name	Type	(byte)	Description
1.	HIL086R	DAT	1213529	: BCD form of HIL086R : 10 materials, 66n, 22g, P_5 cross sections
2.	BCD2BIN	FOR	1531	: Conversion program of HIL086R from BCD to binary form.
3.	DENSINFO	DAT	3185	: Atomic number densities of 10 materials in HIL086R